Institutionen för systemteknik
Department of Electrical Engineering

**Master's Thesis**

# A Control-Oriented 0D Model of a Turbocharger Gas Stand Including Heat Transfer

Master's Thesis Performed in Vehicular Systems,
The Institute of Technology at Linköping University
by

**Mikael Bengtsson**

LiTH-ISY-EX--15/4849--SE

Linköping 2015

Department of Electrical Engineering
Linköpings universitet
SE-581 83 Linköping, Sweden

Linköpings tekniska högskola
Linköpings universitet
581 83 Linköping

# A Control-Oriented 0D Model of a Turbocharger Gas Stand Including Heat Transfer

Master's Thesis Performed in Vehicular Systems,
The Institute of Technology at Linköping University
by

**Mikael Bengtsson**

LiTH-ISY-EX--15/4849--SE

Supervisors: **Ph.D Andreas Thomasson**
ISY, Linköping University
**Ph.D Oskar Leufvén**
Scania CV AB

Examiner: **Associate Professor Lars Eriksson**
ISY, Linköping University

Linköping, June 10, 2015

**Avdelning, Institution**
Division, Department

Institutionen för systemteknik
Department of Electrical Engineering
SE-581 83 Linköping

**Datum**
Date

2015-06-10

**Språk**
Language

☐ Svenska/Swedish
☒ Engelska/English
☐ ________________

**Rapporttyp**
Report category

☐ Licentiatavhandling
☒ Examensarbete
☐ C-uppsats
☐ D-uppsats
☐ Övrig rapport
☐ ________________

**ISBN**
—

**ISRN**
LiTH-ISY-EX--15/4849--SE

**Serietitel och serienummer**
Title of series, numbering

**ISSN**
—

**URL för elektronisk version**
`http://urn.kb.se/resolve?urn=urn:nbn:se:liu:diva-XXXXX`

**Titel**
Title: A Control-Oriented 0D Model of a Turbocharger Gas Stand Including Heat Transfer

**Författare**
Author: Mikael Bengtsson

**Sammanfattning**
Abstract

A turbocharger's performance is measured in a gas stand in order to provide information of the components characteristics. The measurement procedure is a very time consuming process and it is thus desired to make it more time-efficient.

To allow for development of an enhanced control strategy used during the measurements, a 0D model of a gas stand is developed. The physical gas stand components are modeled and validated against measurements, all showing a reasonable result. Turbocharger heat transfers are investigated and modeled using a lumped capacitance approach. The heat transfer models shows approximative results when comparing with measurements which is explained by the lack of temperature measurement made on the bearing housing.

When the complete gas stand model is validated against measurements, an improvement of the measurement procedure is examined. By adding an idealized heat source with the possibility to heat the compressor housing, it is possible to reduce the time it takes to reach an equilibrium when switching between two steady state operating points.

**Nyckelord**
Keywords: turbocharger, gas stand, heat transfer

# Abstract

A turbocharger's performance is measured in a gas stand in order to provide information of the components characteristics. The measurement procedure is a very time consuming process and it is thus desired to make it more time-efficient.

To allow for development of an enhanced control strategy used during the measurements, a 0D model of a gas stand is developed. The physical gas stand components are modeled and validated against measurements, all showing a reasonable result. Turbocharger heat transfers are investigated and modeled using a lumped capacitance approach. The heat transfer models shows approximative results when comparing with measurements which is explained by the lack of temperature measurement made on the bearing housing.

When the complete gas stand model is validated against measurements, an improvement of the measurement procedure is examined. By adding an idealized heat source with the possibility to heat the compressor housing, it is possible to reduce the time it takes to reach an equilibrium when switching between two steady state operating points.

# Acknowledgments

First I would like to thank my examiner Lars Eriksson and my supervisor Andreas Thomasson at Vehicular Systems. Your advice and support throughout the thesis have been of great use.

I would also like to thank Erik Halldorf, head of NMGG - Gas Exchange System and Turbocharger Development, for giving me this opportunity. I have really enjoyed my time at Scania. Lastly, I would like to express my gratitude towards my supervisor Oskar Leufvén. You have always been patient and helped me solve my problems with your great expertise, for that I am thankful.

*Södertälje, June 2015*
*Mikael Bengtsson*

# Contents

**1 Introduction** **1**
1.1 Purpose and Goal . . . 2
1.2 Related Research . . . 2

**2 Measurements** **5**
2.1 Test Facility . . . 5
2.2 Test Procedure . . . 6

**3 Modeling** **9**
3.1 Compressor . . . 9
  3.1.1 Compressor flow model . . . 10
  3.1.2 Compressor efficiency model . . . 12
3.2 Friction . . . 14
3.3 Turbine . . . 16
  3.3.1 Turbine flow model . . . 16
  3.3.2 Turbine efficiency model . . . 17
3.4 Turbocharger Dynamics . . . 18
3.5 Butterfly Valve . . . 18
3.6 Burner . . . 20
3.7 Control Volume . . . 23
3.8 Intercooler . . . 23
3.9 Heat Transfer . . . 23
  3.9.1 Convection between gas and turbine . . . 25
  3.9.2 Conduction between turbine and bearing housing . . . 26
  3.9.3 External heat loss of turbine . . . 27
  3.9.4 Conduction between bearing housing and compressor . . . 28
  3.9.5 Convection between gas and compressor . . . 29
  3.9.6 External heat loss of compressor . . . 31
  3.9.7 Convection between bearing housing and oil . . . 32
  3.9.8 Convection between bearing housing and water . . . 34
  3.9.9 Thermal mass . . . 35
3.10 Complete Model Validation . . . 36

**4 Control** **39**

**5 Conclusions and Future Work** **41**

**A Appendix** **45**

**Notation** **51**

**Bibliography** **55**

# 1

# Introduction

The last decades the use of turbochargers has been widely extended in the automotive industry. With tightened legislation around emissions, engine developers are constantly forced to increase efficiency in order to meet the new restraints. A turbocharger is considered a big contributor in this process since it recovers otherwise wasted thermal and kinetic energy from the exhaust gases. An added turbocharger allows for engine down-sizing which in principle means maintaining the same power with a lighter, supercharged engine. With less weight to carry, the natural result is a reduced fuel consumption.

When purchasing a turbocharger, manufacturers generally enclose performance maps of the compressor and turbine respectively. The maps are measured by the manufacturers themselves and show the relation between pressure ratio, mass flow rate, efficiency and turbocharger speed. Good knowledge of a turbocharger's characteristic is essential when optimising engine control strategies, making the accuracy of the maps crucial. Hence, complementary tests are often performed by engine developers to ensure the maps correctness.

The performance of a turbocharger is determined in a test rig usually referred to as a gas stand. A test procedure involves delivery of hot pressurised gas driving the turbine, normally produced by a mechanical compressor coupled with a burner. The compressor mass flow is simultaneously restrained with a control valve downstream the compressor. With this arrangement pressure ratios, turbine inlet temperature and turbocharger speed can be controlled individually. The maps are produced by measuring steady state operating points throughout predefined speed lines, where compressor surge and choke defines the outer boundaries of each line.

## 1.1 Purpose and Goal

Since testing a turbocharger is a time consuming and thus costly procedure, it is of interest to make it more efficient. This thesis aims to develop a 0D model of a test stand in order to allow for development of an enhanced control strategy used when mapping a turbocharger. Conventional control are carried out with the help of basic PID controllers and it is to be examined if an improved method can be obtained. With the help of mathematical models describing the physical processes well, it is possible to work out new intelligent strategies in a simulation environment instead of using trial and error on the physical gas stand.

One main task is to model the thermodynamics occurring in a gas stand with focus put on the turbocharger. The turbine is driven by hot exhaust gases and working temperatures can easily exceed $800°C$, resulting in heat transfers throughout the whole component. Since the most time consuming part of a steady state measurement is to wait for the turbocharger to reach a thermal equilibrium, a lot of time would be spared if it is possible to reduce the settling time in some way.

Test stand measurements are often carried out without full covering of turbine work conditions, explained by the fact that compressor surge sets the limit. Complete knowledge of a turbine's performance is of interest and one solution to allow for that is a closed loop configuration on the compressor side. Practically, this means that the pressurized air leaving the compressor outlet is led back to the compressor inlet, with an intercooler and a control valve in between. The objective is to incorporate this arrangement in the gas stand model.

## 1.2 Related Research

General knowledge of turbocharger test facilities is required to understand the essential components and their purpose. Several papers describe the development process of test facilities and a few variations in configuration appear. Young and Penz [1990] designed a test facility capable of running several turbocharger tests simultaneously. The test stands were built with independent gas circuits (2-loop), see SAE J1826 [1995] for a closer description. A burner fed with natural gas was used, delivering a turbine inlet temperature of maximum $815°C$. Venson et al. [2006] constructed a gas stand using the 1-loop configuration, i.e. the compressor output flow was led to the turbine intake with a burner in between.

Stemler and Lawless [1997] introduced a test facility designed for transient performance measurement of larger diesel turbochargers. A test stand mainly consisting of a burner and a screw compressor was the final product, operating at a maximum temperature of $648°C$. The same configuration was used by Naundorf et al. [2001] with the discrepancy of a double fluted hot gas generator, permitting increased precision when controlling the turbine inlet temperature. The arrangement allowed temperatures up to $1050°C$.

Instead of a burner, Luján et al. [2002] used a diesel engine to deliver hot gas to drive the turbine of a decoupled turbocharger, hence making performance measurements possible. Leufven and Eriksson [2010] on the other hand developed a method to bench engine mounted turbochargers by adding an extra throttle upstream of the first compressor stage, thus extending the interval of obtainable corrected mass flows in the compressor.

Even though the actual working environment of a turbocharger includes hot temperatures, test facilities using cold air exists as well. This is explained by the simple fact that they are less expensive and more user friendly. Both Filho et al. [2002] and Uhlenhake et al. [2011] developed test stands using cold air only. At the University of Genoa, Capobianco and Marelli [2005] used an electrical heater to slightly raise the temperature of the compressed air delivered to the turbine, hence avoiding freezing conditions. The facility also incorporated a pulse generator allowing simulated exhaust conditions.

The study shows that variations exist, although the main configuration seems to be a test stand consisting of, apart from other necessary components such as control valves and pipes, a screw compressor and a burner allowing measurements at higher working temperatures.

Traditionally, turbochargers have been modeled with the assumption of adiabatic processes occurring throughout the component. The general opinion nowadays is that heat transfer has a significant impact on turbocharger efficiency and needs to be taken into account to obtain accurate performance maps. Different approaches to model the heat transfers have been discussed where the most established method is to apply a one-dimensional model with lumped capacitances. This is done in several papers with Romagnoli and Martinez-Botas [2012], Olmeda et al. [2013] and Serrano et al. [2014] as examples, where the turbocharger is divided into varying number of sections simplified as cylinders in the calculations.

# 2

# Measurements

All measurements used in this thesis were conducted at the Saab Powertrain facilities in Trollhättan just before the company was declared bankrupt. This chapter describes both the test facility with its major components as well as the different measurements carried out.

## 2.1 Test Facility

The gas stand equipment in Trollhättan consists of two variable screw compressors from Atlas Copco delivering pressurized air, led through a large air-to-water intercooler, with the possibility of feeding both the compressor and turbine inlet. A diesel burner is used to increase temperature of the pressurized air, thus simulating hot exhaust gases. Individually controllable water and oil circuits with adjustable feeding pressure and fluid temperatures are led through the turbochargers. Two butterfly valves, one downstream the compressor and one downstream the turbine, operate as restrictions and allows for control of pressure ratios over the compressor and turbine respectively. The surrounding room is climate controlled and the ambient temperature is roughly $20^{\circ}C$ during the conducted measurements. A schematic overview of the test facility can be seen in Figure 2.1 and photos of the actual test rig are shown in Figure 2.2 and Figure 2.3.

The test rig is fully equipped with all sensors needed for mapping a turbo, thus referring to the pressure, flow, temperature and speed sensors found in Figure 2.1. In addition to that, twelve extra surface temperature sensors are positioned around the turbocharger with six on the compressor scroll and back plate, three on the compressor inlet pipe, one on the compressor outlet pipe and two on the turbine housing.

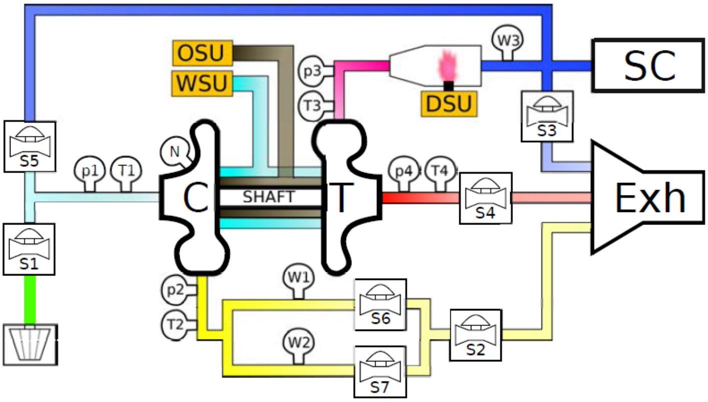

*Figure 2.1: A schematic overview of the gas stand in Trollhättan. Used abbrevations: SC - Screw Compressors, S - Control Valve, Exh - Exhaust Pipe, DSU/OSU/WSU - Diesel/Oil/Water Supply Unit. The symbols p, T, W, and N indicate measurement locations. The picture is taken from Leufven [2013] with permission.*

Two v-cone differential pressure measurement rings are used for different ranges of flow on the compressor side ($W1$ and $W2$ in Figure 2.1). The flow is alternated between the two v-cones with the help of control valves $S6$ and $S7$.

Regarding the water and oil circuits, flow measurements and temperature measurements before and after passing the turbocharger are available for each circuit respectively.

## 2.2 Test Procedure

Measurements on three different turbochargers were carried out during the testing period in Trollhättan. The available data consists mainly of steady-state measurements and only one of the turbochargers, a Mitsubishi TD04HL-15T, includes time-resolved measurement data. Since time-resolved data will allow for a complete model validation later on, the TD04HL-15T is chosen as the turbocharger to represent with models.

As mentioned in the introduction, a normal test procedure of a turbocharger includes steady state measurements throughout a couple of speed lines, where compressor choke and surge sets the outer boundaries for each line. Similar measurements were of course conducted on the Mitsubishi TD04HL-15T, but some additional tests were also carried out. All measurements together with a brief description can be found in the list below:

- **Compressor stand still restriction** measured with a locked turbocharger shaft and the compressed air supply connected to the compressor inlet.

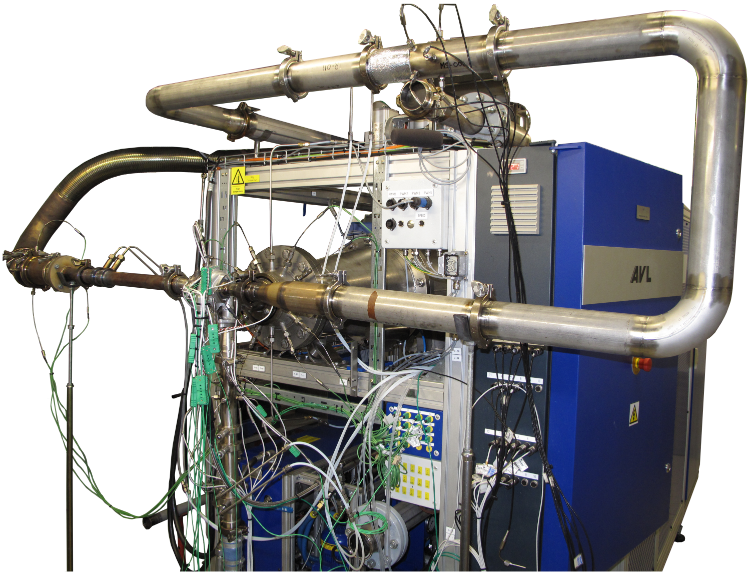

*Figure 2.2: An overview of the gas stand. All components are fitted in the rig with exception for the intercoolers and screw compressors which are placed in another room.*

- **Compressor restriction map** conducted with the gas stand fresh compressed air supply connected to the compressor inlet. Pressure ratios of $\Pi_c < 1$ were measured at constant speeds.
- **Adiabatic map**, i.e. measurements done with minimized heat transfer, were carried out while matching the compressor housing temperature to the compressor outlet temperature with help of the oil and water circuits.
- **Hot map** measurements carried out with a normal test procedure with varying turbine inlet temperatures $T_{03}$ reaching up to a temperature of $750°C$.
- **Choke flow** measurements for a number of speeds conducted with a fully opened butterfly valve downstream the compressor.
- **Medium hot map** measurements with turbine inlet temperatures of $300°C$ and $450°C$, conducted with a normal test procedure with varying oil and water temperatures.
- **Step responses** with steps made in turbocharger speed, measured with a fixed butterfly valve position.

The turbocharger and adjacent pipes were insulated during all conducted measurements in order to reduce the external heat transfers. The steady state and time-resolved measurement data can be seen in Figure A.1 and Figure A.2 (found in Appendix A).

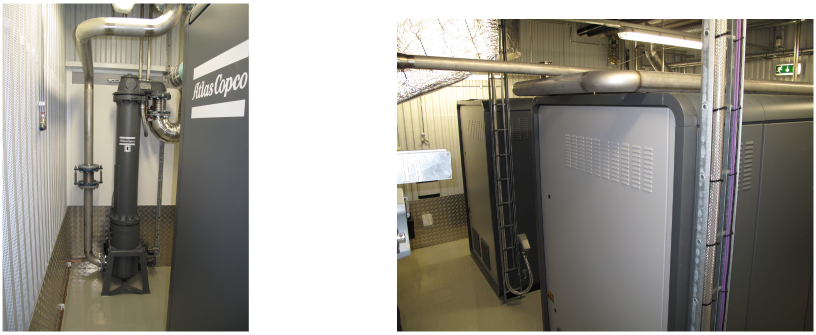

***(a)*** *Screw compressor.*

***(b)*** *Air-to-water intercoolers.*

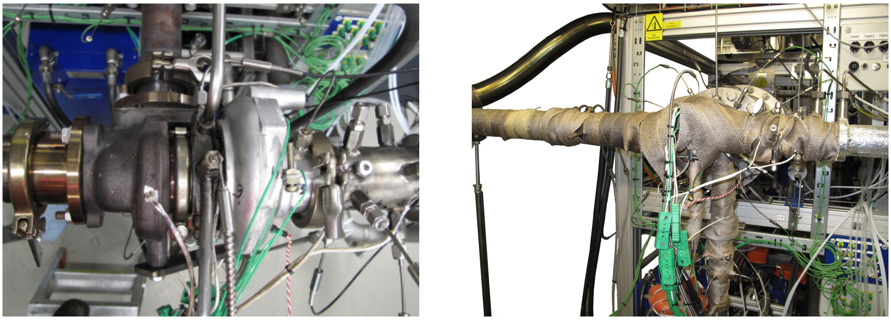

***(c)*** *Installation overview.*

***(d)*** *Insulated turbocharger and adjacent pipes.*

***Figure 2.3:*** *Photos of the actual gas stand in Trollhättan.*

# 3

# Modeling

This chapter describes the modeling process of each gas stand component respectively. After validation against measurements, all models are integrated in Simulink and a complete model validation, comparing measured and simulated data, sums it up. The fundamentals as well as used parameters are briefly explained in each section in order to allow for a better understanding of the models.

## 3.1 Compressor

The compressor uses power provided by the shaft and compresses the passing fluid, consequently increasing fluid pressure and temperature. The compressor power can be defined by the first law of thermodynamics applied on a steady flow control volume as

$$\dot{W}_c = \dot{m}_c(h_{02} - h_{01}) + \dot{Q}_c = [c_{p,c}\ constant] = \dot{m}_c c_{p,c}(T_{02} - T_{01}) + \dot{Q}_c \tag{3.1}$$

where $\dot{m}_c$ is the compressor mass flow, $h_{01}$ and $h_{02}$ are the inlet and outlet specific enthalpy, respectively, $c_{p,c}$ is the specific heat capacity at constant pressure, $T_{01}$ is the compressor inlet temperature and $T_{02}$ is the compressor outlet temperature. The heat transfer $\dot{Q}_c$ is generally not considered when describing the compression process in turbochargers, but since one main objective in this thesis is to determine the heat transfers, it is obviously included.

Adiabatic compressor efficiency $\eta_{c,adi}$ is defined as the ratio between the power required by an ideal isentropic process and actual power consumed, expressed as

$$\eta_{c,adi} = \frac{\dot{W}_{c,ideal}}{\dot{W}_c} = \frac{\left(\frac{p_{02}}{p_{01}}\right)^{\frac{\gamma_c-1}{\gamma_c}} - 1}{\frac{T_{02}}{T_{01}} - 1} \tag{3.2}$$

where $\gamma_c$ is the heat capacity ratio, $p_{01}$ is the compressor inlet pressure and $p_{02}$ is the compressor outlet pressure.

The compressor pressure ratio used in the models is defined as

$$\Pi_c = \frac{p_{02}}{p_{01}} \tag{3.3}$$

The compressor maps are represented with corrected compressor mass flow $\dot{m}_{c,co}$ and corrected speed $N_{tc,co}$, both normalized against ambient conditions and defined as

$$\dot{m}_{c,co} = \dot{m}_c \frac{\sqrt{T_{01}/T_{c,ref}}}{\left(p_{01}/p_{c,ref}\right)} \qquad and \qquad N_{tc,co} = \frac{N_{tc}}{\sqrt{T_{01}/T_{c,ref}}} \tag{3.4}$$

where $N_{tc}$ is the turbocharger rotational speed. Used reference states are $T_{c,ref} = 20°C$ and $p_{c,ref} = 1\ atm$.

### 3.1.1 Compressor flow model

The compressor flow model aims to estimate a compressor mass flow with a couple of known parameters as

$$\dot{m}_c = f(p_{01}, p_{02}, T_{01}, \omega_{tc}) \tag{3.5}$$

where $\omega_{tc}$ is the turbocharger angular speed.

A model based on the dimensionless quantities $\Psi, \Phi$ and $Ma$, proposed by Tu and Chen [2013] is used. The following parameters are included in the model

$$U_c = \frac{\pi}{60} d_c N_{tc} \tag{3.6}$$

$$\Psi = \frac{c_{p,c} T_{01} \left( \left(\frac{p_{02}}{p_{01}}\right)^{\frac{\gamma_c-1}{\gamma_c}} - 1 \right)}{\frac{1}{2} U_c^2} \tag{3.7}$$

$$\Phi = \frac{\dot{m}_c R T_{01}}{\frac{\pi}{4} d_c^2 U_c p_{01}} \tag{3.8}$$

$$Ma = \frac{U_c}{\sqrt{\gamma_c R T_{01}}} \tag{3.9}$$

where $U_c$ is the compressor blade tip speed, $R$ is the ideal gas constant and $d_c$ is the compressor diameter. The model is defined as

$$\Phi = a + (1 - e^{\Psi^c + b}) \tag{3.10}$$

where $a$, $b$ and $c$ are functions of the Mach number as

$$a = a_n Ma^n + a_{n-1} Ma^{n-1} + \ldots + a_1 Ma + a_0 \tag{3.11}$$

$$b = b_n Ma^n + b_{n-1} Ma^{n-1} + \ldots + b_1 Ma + b_0 \tag{3.12}$$

$$c = c_n Ma^n + c_{n-1} Ma^{n-1} + \ldots + c_1 Ma + c_0 \tag{3.13}$$

A measurement series including the highest measured turbocharger speed is used to estimate the constants $a_0 - a_n$, $b_0 - b_n$ and $c_0 - c_n$ with least squares. The resulting model fit is presented in Figure 3.1 with used polynomial order of $n = 7$. The model captures the flow characteristic well at lower turbocharger speeds but deteriorates with increased speed. A compressor flow model of a more complex nature would most probably result in a better fit. However, the model used here is considered sufficient since it gives a rough estimation for all speeds.

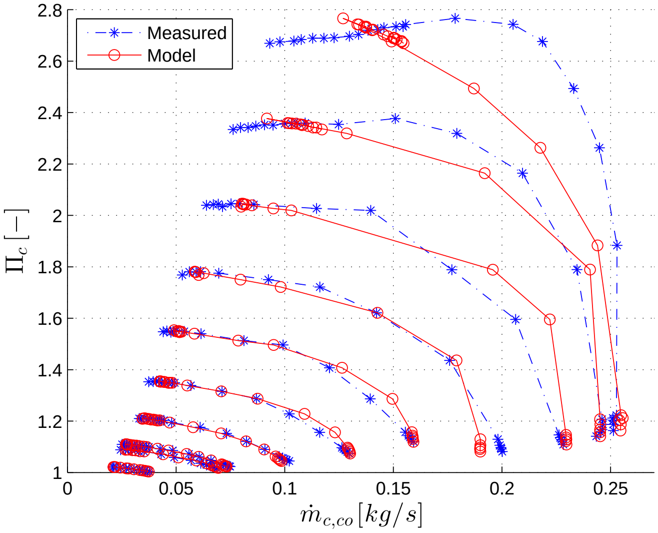

***Figure 3.1:*** *Corrected compressor mass flow versus compressor pressure ratio for a number of turbocharger speeds. The model fit is worse for higher speeds but the model still gives a rough estimation of the quantity.*

### 3.1.2 Compressor efficiency model

To make quantification of the compressor heat transfer $\dot{Q}_c$ possible, the compressor efficiency model is constructed using adiabatic measurements only, hence $\dot{Q}_c \approx 0$ in Eq. (3.1). In other words it can be described as the aerodynamic compressor efficiency.

Since the adiabatic measurements only range up to a maximum corrected speed of $N_{tc,co} = 113\,000\, rpm$, the lines representing the three highest speeds are from a map measured without matching the compressor housing and compressed air temperature, making heat transfer between fluid and housing possible. This is done to allow for simulation at higher speeds. Although, a better alternative would possibly be to extrapolate the speed lines measured under adiabatic circumstances instead. As a result of this, all heat transfer calculations are done with corrected speeds less or equal to $113\,000\, rpm$.

A first modeling attempt is made using the quadratic form compressor efficiency model proposed by Eriksson and Nielsen [2014], defined in Eq. (3.14)-(3.18) where $r_c$ is the compressor radius. The constants $\eta_{c,max}$, $\dot{m}_{c,co@\eta_{c,max}}$, $\Pi_{c@\eta_{c,max}}$, $Q_{11}$, $Q_{12}$ and $Q_{22}$ are estimated using least squares. The resulting model fit can be seen in Figure 3.2.

$$\Pi_{c,max} = \left( \frac{u_2^2 \Psi_{max}}{2 c_{p,c} T_{01}} + 1 \right)^{\frac{\gamma_c}{\gamma_c - 1}} \tag{3.14}$$

$$\dot{m}_{c,co} = \dot{m}_{c,co_{max}} \sqrt{1 - \left( \frac{\Pi_c}{\Pi_{c,max}} \right)^2} \tag{3.15}$$

$$\dot{m}_c = \dot{m}_{c,co} \frac{p_{01}/p_{c,ref}}{\sqrt{T_{01}/T_{c,ref}}} \tag{3.16}$$

$$u_2 = r_c \omega_c = 2\pi r_c N_{tc} = 2\pi r_c N_{tc,co} \sqrt{T_{01}/T_{c,ref}} \tag{3.17}$$

$$\eta_{c,adi} = \eta_{c,max} - \begin{bmatrix} \dot{m}_{c,co} - \dot{m}_{c,co@\eta_{c,max}} \\ \sqrt{\Pi_c - 1} - \left( \Pi_{c@\eta_{c,max}} - 1 \right) \end{bmatrix}^T \begin{bmatrix} Q_{11} & Q_{12} \\ Q_{12} & Q_{22} \end{bmatrix} \begin{bmatrix} \dot{m}_{c,co} - \dot{m}_{c,co@\eta_{c,max}} \\ \sqrt{\Pi_c - 1} - \left( \Pi_{c@\eta_{c,max}} - 1 \right) \end{bmatrix} \tag{3.18}$$

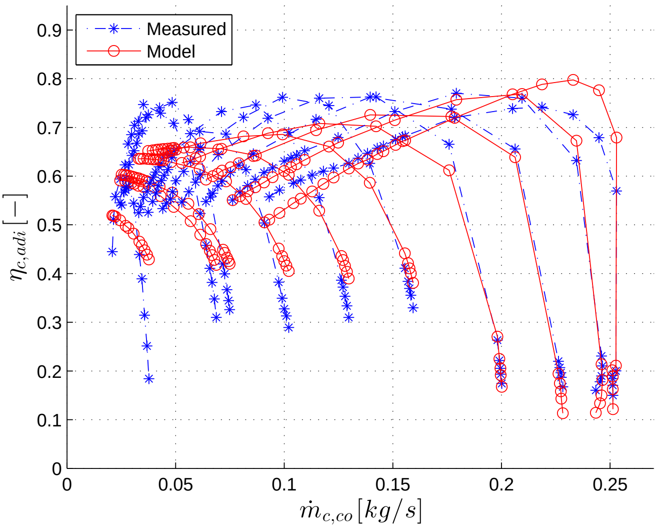

***Figure 3.2:*** *Quadratic form compressor efficiency model versus measurements. The model fit is not considered sufficient, hence another method is required.*

Since the adiabatic compressor efficiency will play a major role in the process of determining the compressor heat transfer, the model fit seen in Figure 3.2 is not considered good enough. Instead a function is constructed in Matlab, where each speed line is manually extended with start and end values and represented by a polynomial with the help of a least squares method. By using linear interpolation along the speed, the script calculates an estimated efficiency as

$$\eta_{c,adi} = f(\dot{m}_{c,co}, N_{tc,co}) \tag{3.19}$$

The fitted polynomials for all speed lines are shown in Figure 3.3 and it can easily be concluded that the provided result is better compared to the quadratic form model. Although, at higher speeds ($N_{tc,co} > 96\,000\,rpm$) the measured data is difficult to represent as polynomials which leads to worse results.

When implemented in Simulink, a minimum compressor efficiency of $\eta_{c,adi} = 0.05$ is set with the purpose of avoiding a singularity when calculating the adiabatic compressor power.

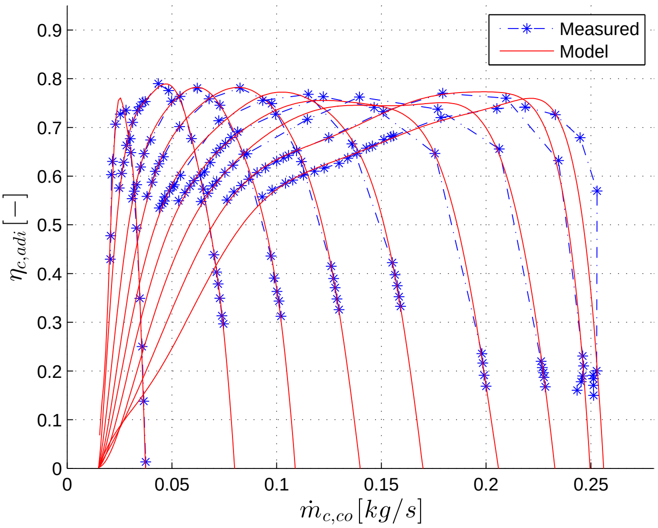

***Figure 3.3:*** *Developed adiabatic compressor efficiency model versus measurements. The model shows a better fit compared to the quadratic form efficiency model. Corrected speeds* $N_{tc,co}$ *from left to right: 22000, 44000, 61000, 78000, 96000, 113000, 130000, 147000, 164000 [rpm].*

## 3.2 Friction

The turbocharger shaft is held in place by a thrust bearing and a radial bearing. Petroff's Law for bearing frictional torque is defined as

$$Tq_f = \frac{\pi}{4}\frac{\mu_{oil} L_b D_b^3}{\epsilon_r}\omega_{tc} \tag{3.20}$$

where $\mu_{oil}$ is the dynamic oil viscosity, $\epsilon_r$ is the fluid film thickness and $L_b$ and $D_b$ are the bearing length and diameter. Likewise Petroff's law, it is assumed that the frictional torque is proportional to the dynamic oil viscosity with proposed model as

$$\dot{W}_f/\omega_{tc} = Tq_f = (c_0 + c_1\omega_{tc})\cdot\mu_{oil}, \qquad \mu_{oil} = \nu_{oil}\rho_{oil} \tag{3.21}$$

where $\dot{W}_f$ is the friction power. The kinematic viscosity $\nu_{oil}$ and density $\rho_{oil}$ are both dependent on oil temperature with their relationships shown in Figure A.3.

Using cold measurements where the whole turbocharger has a uniform temperature equal to the ambient, i.e. $T_c \approx T_{bh} \approx T_t \approx T_{amb}$, leads to the conclusion that the only heat transfer occurring in the turbo is the converted friction power, $\dot{Q}_f = \dot{W}_f$. Since the bearing housing temperature is not increased despite of the added energy, one can assume that the heat contributed by the friction power must be transferred to the oil and water, hence

$$\dot{Q}_f = \dot{Q}_{oil} + \dot{Q}_{wat} \tag{3.22}$$

where the heat transferred to the oil and water, $\dot{Q}_{oil}$ and $\dot{Q}_{wat}$, can be determined by measured quantities, see Eq. (3.72) and Eq. (3.74). With the friction power quantified and by assuming constant oil temperature, the constants $c_0$ and $c_1$ are estimated using least squares. The resulting model fit is shown in Figure 3.4.

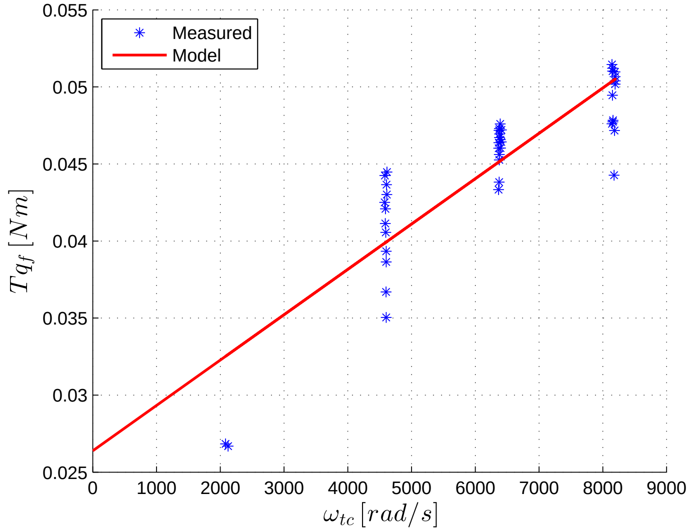

***Figure 3.4:*** *Friction torque versus angular velocity for a constant oil temperature. The linear relation found in the figure validates that the method used is reasonable.*

As expected, the estimated friction torque have an approximate linear relationship to the angular speed and the linear model represent the measurements roughly.

## 3.3 Turbine

The turbine extracts energy from the fluid and transforms it into power delivered to the shaft. While passing through the turbine, the gas expands and fluid pressure and temperature drops. By applying the same principle as for the compressor, a steady flow control volume around the turbine yields

$$\dot{W}_t = \dot{m}_t(h_{03} - h_{04}) + \dot{Q}_t = [c_{p,t}\ constant] = \dot{m}_t c_{p,t}(T_{03} - T_{04}) + \dot{Q}_t \tag{3.23}$$

where $\dot{m}_t$ is the turbine mass flow, $h_{03}$ and $h_{04}$ are the inlet and outlet specific enthalpy, respectively, $c_{p,t}$ is the specific heat capacity at constant pressure, $T_{03}$ is the turbine inlet temperature and $T_{04}$ is the turbine outlet temperature.

Ideal turbine power is defined as the power required by an isentropic process as

$$\dot{W}_{t,ideal} = \dot{m}_t c_{p,t} T_{03} \left\{ \left(1 - \frac{p_{04}}{p_{03}}\right)^{\frac{\gamma_t - 1}{\gamma_t}} \right\} \tag{3.24}$$

where $\gamma_t$ is the heat capacity ratio, $p_{03}$ is the turbine inlet pressure and $p_{04}$ is the turbine outlet pressure. The turbine efficiency $\eta_t$ is defined by the ratio of actual power produced and power utilized by an ideal process, stated in Eq. (3.25) below. The actual power produced is defined by the added adiabatic compressor power and friction power.

$$\eta_t = \frac{\dot{W}_t}{\dot{W}_{t,ideal}} = \frac{\dot{W}_{c,adi} + \dot{W}_f}{\dot{m}_t c_{p,t} T_{03} \left\{ \left(1 - \frac{p_{04}}{p_{03}}\right)^{\frac{\gamma_t - 1}{\gamma_t}} \right\}} \tag{3.25}$$

The turbine pressure ratio is defined as

$$\Pi_t = \frac{p_{03}}{p_{04}} \tag{3.26}$$

### 3.3.1 Turbine flow model

Instead of the corrected parameters used to represent the compressor maps, turbine maps often use *turbine flow parameter* (TFP), defined as

$$TFP = \dot{m}_t \frac{\sqrt{T_{03}}}{p_{03}} \tag{3.27}$$

The turbine flow model used is proposed by Eriksson and Nielsen [2014], expressed in Eq. (3.28). With measurement data of varying turbine inlet temperatures, the constants $TFP_{max}$ and $TFP_{exp}$ are estimated using least squares. The resulting model fit is shown in Figure 3.5, which validates that the model represent the measurements well.

$$TFP = TFP_{max} \sqrt{1 - \left(\frac{1}{\Pi_t}\right)^{TFP_{exp}}} \tag{3.28}$$

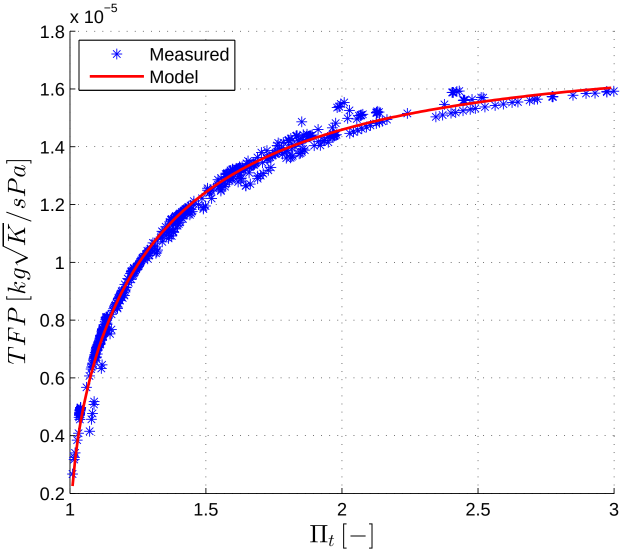

***Figure 3.5:*** *Turbine flow model versus measurements. The model fit shows that the model used is decent.*

### 3.3.2 Turbine efficiency model

The turbine efficiency model used is proposed by Watson and Janota [1982] and includes the *blade speed ratio* ($BSR$). The authors state that turbine efficiency peaks at $BSR = 0.7$ and the parameter $BSR_{opt}$ is thus set likewise. The model is defined as

$$BSR = \frac{\omega_{tc} r_t}{\sqrt{2c_{p,t} T_{03} \left(1 - \Pi_t^{\frac{\gamma_t - 1}{\gamma_t}}\right)}} \tag{3.29}$$

$$\eta_t(BSR) = \eta_{t,max} \cdot \left\{1 - \left(\frac{BSR - BSR_{opt}}{BSR_{opt}}\right)^2\right\} \tag{3.30}$$

where $r_t$ is the turbine radius. The efficiency $\eta_t$ is given by Eq. (3.25) and the constant $\eta_{t,max}$ is estimated using least squares with measurements of varying turbine inlet temperatures. The resulting model fit can be seen in Figure 3.6.

Since all measurements are found within a narrow range in BSR, the model is developed largely by means of an assumption. When comparing model and measurements, the model at least seems to follow the main trend but it is difficult to conclude anything else. Hence, the complete model validation will tell if the proposed turbine efficiency model is adequate.

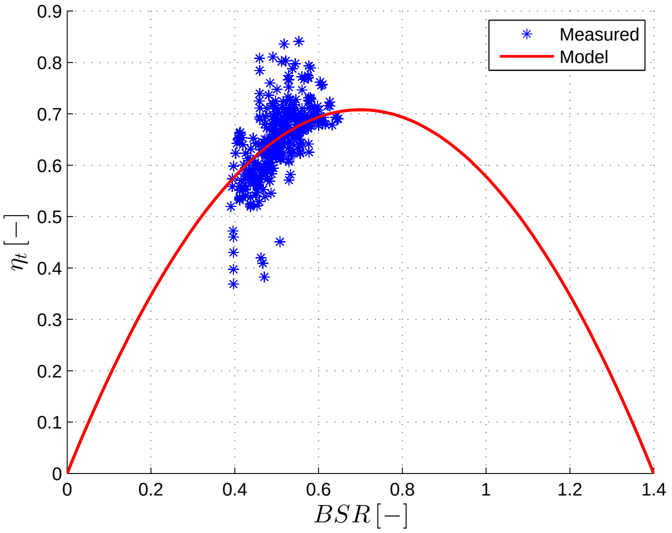

***Figure 3.6:*** *Turbine efficiency model versus measurements shows that the model catches the main trend recognized in the measurement data.*

## 3.4 Turbocharger Dynamics

To include the turbocharger dynamics, Newton's second law is applied on the shaft connecting the turbine and compressor, expressed as

$$\frac{d\omega_{tc}}{dt} = \frac{1}{J_{tc}\omega_{tc}}\left(\dot{W}_t - \dot{W}_c - \dot{W}_f\right), \qquad J_{tc} = 2.55 \cdot 10^{-5}\, kgm^2 \tag{3.31}$$

where the moment of inertia $J_{tc}$ for a Mitsubishi TD04HL-15T rotor is measured by Westin [2002]. When implemented in Simulink, a lower saturation limit of the angular speed is set in order to avoid division by zero.

Equation (3.32) represent an energy balance with a control volume around the shaft valid at steady state operating points.

$$\dot{W}_t = \dot{W}_c + \dot{W}_f \tag{3.32}$$

## 3.5 Butterfly Valve

Butterfly valves are commonly used components in the automotive industry, e.g. functioning as throttles in combustion engines. In the gas stand it is found operating as a variable restriction downstream the compressor. A model proposed by Eriksson and Nielsen [2014] is used to represent the component. The model takes compressible flow into account and returns an estimated mass flow with given parameters such as the pressure before and after the valve, $p_{bef,bv}$ and $p_{aft,bv}$, the outlet temperature $T_{aft,bv}$ and the valve position $\alpha$. The following equations defines the model

$$\Pi(\frac{p_{aft,bv}}{p_{bef,bv}}) = \max\left(\frac{p_{aft,bv}}{p_{bef,bv}}, \left(\frac{2}{\gamma_c + 1}\right)^{\frac{\gamma_c}{\gamma_c - 1}}\right) \tag{3.33}$$

$$\Psi_0(\Pi) = \sqrt{\frac{2\gamma_c}{\gamma_c - 1}\left(\Pi^{\frac{2}{\gamma_c}} - \Pi^{\frac{\gamma_c+1}{\gamma_c}}\right)} \tag{3.34}$$

$$\Psi_{li} = \begin{cases} \Psi_0(\Pi) & \text{if } \Pi_{bv} \leq \Pi_{li} \\ \Psi_0(\Pi_{li})\frac{1-\Pi}{1-\Pi_{li}} & \text{otherwise} \end{cases} \tag{3.35}$$

$$\dot{m}_{bv}\left(\alpha, p_{bef,bv}, p_{aft,bv}, T_{bef,bv}\right) = \frac{p_{bef,bv}}{\sqrt{RT_{bef,bv}}} A_{bv}(\alpha) c_{d,bv}(\alpha) \Psi_{li}\left(\frac{p_{aft,bv}}{p_{bef,bv}}\right) \tag{3.36}$$

where the area $A_{bv}$ and drag coefficient $c_{d,bv}$ are represented as a polynomial shown in Eq. (3.37) below.

$$A_{bv} c_{d,bv} = c_0 + c_1\alpha + c_2\alpha^2 + c_3\alpha^3 \tag{3.37}$$

Since pressure nor temperature measurements are available in the closest surroundings of the butterfly valve, a couple of assumptions needs to be done in order to estimate the model constants. The measurement setup downstream the compressor consists of two v-cone flow meters of different size, positioned just before the butterfly valve (see Figure 2.1 for an overview). The flow meters are alternated depending on the compressor mass flow rate and data of the pressure drop over used v-cone is available in the measurements. Assuming that no pressure loss occurs in the pipe from the $p_{02}$ measurement to the v-cone manifold, the pressure before the butterfly valve can be defined as

$$p_{bef,bv} = p_{02} - \Delta p_{v-cone} \tag{3.38}$$

where $\Delta p_{v-cone}$ is the pressure drop over used v-cone. Downstream the butterfly valve the gases are led out through an exhaust pipe which is assumed to be acting as a restriction with linear relationship to the compressor mass flow as

$$p_{aft,bv} = p_{amb}\left(1 + c \cdot \dot{m}_c\right) \tag{3.39}$$

where $p_{amb}$ is the ambient pressure. The constant $c$ is manually adjusted until the best model fit possible is obtained. The last assumption made is that no heat transfer occurs downstream the compressor, hence

$$T_{bef,bv} = T_{02} \tag{3.40}$$

With mentioned assumptions, the constants $c_0, c_1, c_2$ and $c_3$ in Eq. (3.37) are estimated using least squares with measurements of varying turbine inlet temperatures. The resulting model fit is shown in Figure 3.7.

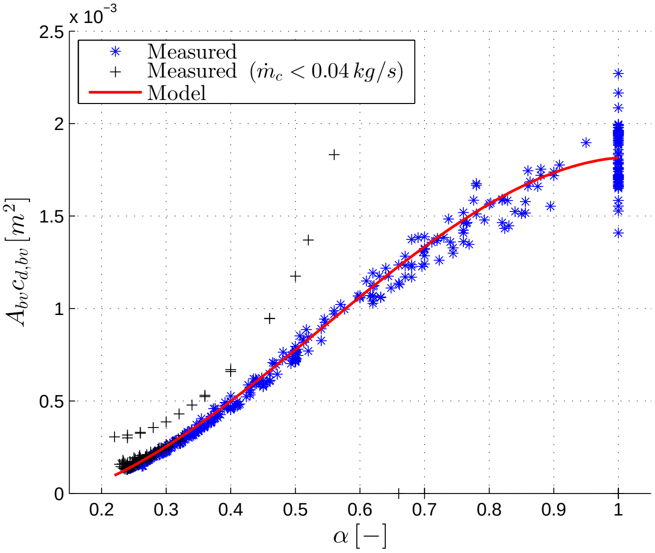

***Figure 3.7:*** *Model fit for the polynomial representing the butterfly valve area and drag coefficient. The poor result is explained by the lack of available measurements nearby the valve. Since the model estimates an approximate quantity, it is still used.*

The result seen in Figure 3.7 indicates that the made assumptions are not describing the reality completely. The most probable explanation to the poor model fit is that the two v-cones leads to different pressure losses when used, in addition to the measured pressure difference over them. All outliers seems to be caused by low mass flows and are considered as measurement errors. Despite of the poor fit, the model however indicates the quantity roughly and is thus used.

## 3.6 Burner

The diesel burner increases the temperature of the pressurized air delivered by the screw compressors, thus simulating hot exhaust gases. Since no thermocouples were placed directly before or after the burner during the conducted measurements, it is fairly difficult to model and validate the component. However, during the compressor stand still restriction measurements, the pressurized and conditioned air normally fed to the burner inlet was instead connected to the compressor inlet. It is assumed that the burner inlet temperature $T_{bef,bu}$ holds a constant value determined by the mean value of the temperature $T_{01}$ from the compressor stand still restriction measurement.

By assuming an ideal combustion, i.e. all energy provided by the diesel fuel is transformed into heat, the heat transfer rate can be defined as

$$\dot{Q}_{bu-g} = \dot{m}_{fu} q_{LHV} \tag{3.41}$$

where $\dot{m}_{fu}$ is the mass flow rate of fuel and $q_{LHV}$ is the lower heating value, for diesel approximated as $q_{LHV} = 48 \frac{MJ}{kg}$. The first law of thermodynamics applied on a steady flow control volume with no heat transfer and constant heat capacity $c_{p,c}$ yields

$$\dot{Q}_{bu-g} = \dot{m}_c c_{p,c} \left( T_{aft,bu} - T_{bef,bu} \right) \tag{3.42}$$

where $T_{bef,bu}$ and $T_{aft,bu}$ are the temperature before and after the burner, respectively. Combining Eq. (3.41)-(3.42) yields an expression for the burner outlet temperature as

$$T_{aft,bu} = \frac{\dot{m}_{fu} q_{LHV}}{\dot{m}_c c_{p,c}} + T_{bef,bu} \tag{3.43}$$

Using all measured maps except the compressor stand still restriction measurement, an estimated burner outlet temperature is calculated with Eq. (3.43) and showed in Figure 3.8, also including the turbine inlet temperature $T_{03}$ and the turbine housing temperature $T_t$.

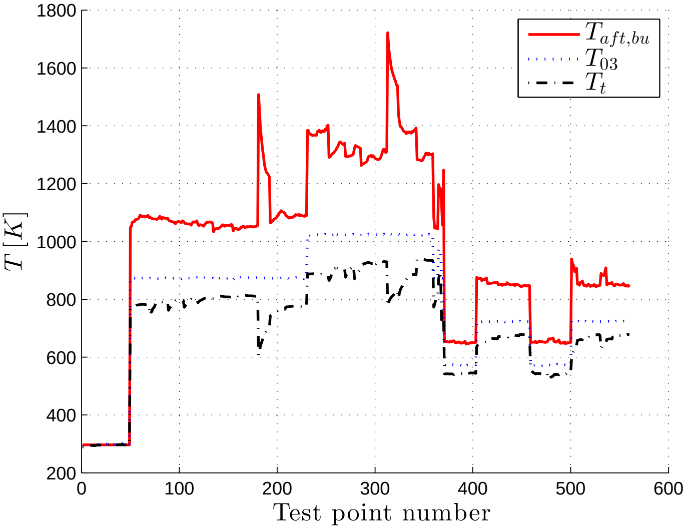

**Figure 3.8:** *The estimated burner outlet temperature $T_{aft,bu}$, turbine inlet temperature $T_{03}$ and turbine housing temperature $T_t$ from steady state measurements. When the turbine housing temperature is decreased, the burner outlet temperature needs to rise in order to maintain the same turbine inlet temperature which explains the relationship seen in the figure.*

The result is considered reasonable since the turbine housing temperature $T_t$ and burner outlet temperature $T_{aft,bu}$ seems to be dependent, cancelling each other out around the turbine inlet temperature $T_{03}$. An explanation to this could be that when the turbine and presumably also the connecting pipes are colder, more energy will be transferred through convection from the gas to the turbine housing, thus making need for the burner to raise the temperature in order to maintain the same turbine inlet temperature $T_{03}$.

The turbine mass flow is assumed to have a linear relationship to the pressure drop over the burner $\Delta p_{bu}$, hence

$$\dot{m}_t = c_0 + c_1 \Delta p_{bu} = c_0 + c_1(p_{bef,bu} - p_{aft,bu}) \tag{3.44}$$

where $p_{bef,bu}$ and $p_{aft,bu}$ are the pressure before and after the burner, respectively. The constants $c_0$ and $c_1$ are estimated using least squares and the model fit is shown in Figure 3.9. The result is satisfying, showing that the model represent a vast majority of the measurements.

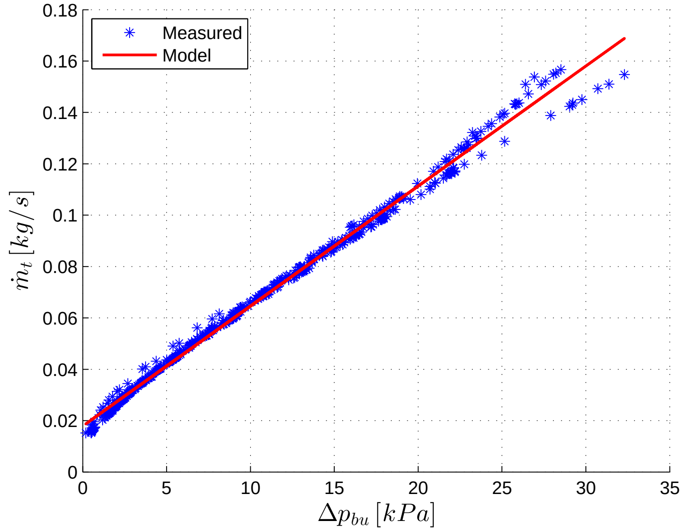

***Figure 3.9:*** *Burner pressure drop model versus measurements shows that the developed model is decent.*

## 3.7 Control Volume

Control volumes refers to the connecting pipes in the gas stand, which are implemented in Simulink as models with temperature $T$ and pressure $p$ as states. The model used is proposed by Eriksson and Nielsen [2014] and defined as

$$\frac{dT}{dt} = \frac{RT}{pVc_v}\left[\dot{m}_{in}c_v(T_{in} - T) + R(T_{in}\dot{m}_{in} - T\dot{m}_{out}) - \dot{Q}\right] \tag{3.45}$$

$$\frac{dp}{dt} = \frac{RT}{V}(\dot{m}_{in} - \dot{m}_{out}) + \frac{p}{T}\frac{dT}{dt} \tag{3.46}$$

where $V$ is the volume, $c_v$ is the heat capacity at constant volume, $\dot{m}_{in}$ and $\dot{m}_{out}$ are the inlet and outlet mass flow, respectively, and $T_{in}$ is the inlet temperature. The model includes heat transfer $\dot{Q}$, although this has not been considered in this thesis.

## 3.8 Intercooler

An intercooler is used in the closed loop circuit to decrease the compressed air temperature before the air is led back to the compressor inlet. Andersson [2005] proposes a model which is defined as

$$\Delta p_{ic} = H\frac{T_{ic,in}\dot{m}_{ic}^2}{p_{ic,in}} \tag{3.47}$$

$$T_{ic,out} = \max\left(T_{cool}, T_{ic,in} + \xi_{ic}\left(T_{ic,in} - T_{cool}\right)\right) \tag{3.48}$$

where $T_{ic,in}$ and $T_{ic,out}$ are the inlet and outlet temperature, respectively, $\dot{m}_{ic}$ is the mass flow, $p_{ic,in}$ is the inlet pressure and $T_{cool}$ is the cooling water temperature. Since no available data exists, some assumptions needs to be done. By assuming a pressure drop of $\Delta p_{ic} = 20\,kPa$ over the intercooler at maximum mass flow, the constant $H$ can be estimated using data from the gas stand measurements. When implemented in Simulink the intercooler effectiveness is set to a constant value of $\xi_{ic} = 0.9$.

## 3.9 Heat Transfer

The quantification of heat transfers in the turbocharger is presented in the following section, where a lumped capacitance model is used to represent the turbocharger and occurring heat transfers. Practically, this means that the turbocharger is divided into three parts consisting of the compressor, bearing housing and turbine. It is assumed that each part holds a uniform temperature dependent on the balance of supplied and abducted energies. An overview of all occurring energy flows in the turbocharger can be seen in Figure 3.10.

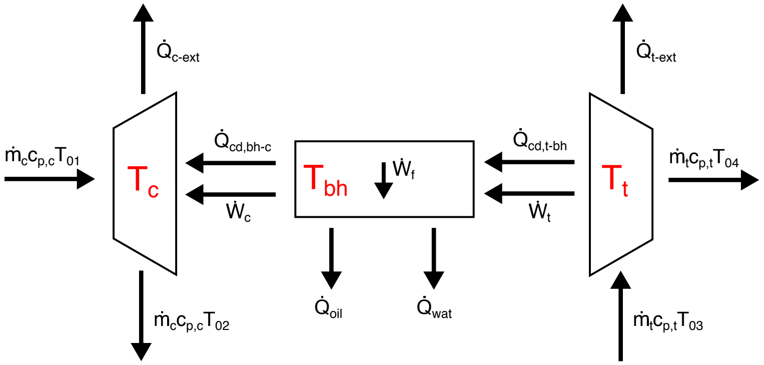
$\dot{Q}_{c\text{-}ext}$
$\dot{Q}_{t\text{-}ext}$
$\dot{m}_c c_{p,c} T_{01}$
$T_c$
$\dot{Q}_{cd,bh\text{-}c}$
$\dot{W}_c$
$T_{bh}$
$\dot{W}_f$
$\dot{Q}_{cd,t\text{-}bh}$
$\dot{W}_t$
$T_t$
$\dot{m}_t c_{p,t} T_{04}$
$\dot{m}_c c_{p,c} T_{02}$
$\dot{Q}_{oil}$
$\dot{Q}_{wat}$
$\dot{m}_t c_{p,t} T_{03}$

***Figure 3.10:*** *Schematic sketch of energies flowing in the turbocharger.* $\dot{Q}_{c-ext}$ *and* $\dot{Q}_{t-ext}$ *represent the total external heat loss in terms of convection, conduction and radiation for the compressor and turbine respectively.*

It is assumed that no heat exchange occurs between the bearing housing and the surroundings. The assumption is motivated by the small surface area exposed to the surroundings and the possible equalization that is done by the radiative and convective heat received from the compressor and turbine housing.

Using the available measurements, the compressor housing temperature $T_c$ and turbine housing temperature $T_t$ are represented as the mean value of all surface temperatures measured on each component respectively. Since no thermocouples were placed on the bearing housing, the bearing housing temperature $T_{bh}$ is instead represented by measurements made on the compressor back plate. This is not unreasonable since the compressor back plate is directly attached to the bearing housing with a large contact area in between. The one, out of three, back plate temperature measurement least affected by the compressor temperature is chosen to represent the bearing housing temperature. The choice is done since it is reasonable to assume that the bearing housing temperature is affected by the turbine, oil and water temperature also, i.e. not mainly by the compressor temperature. For a better understanding, all conducted temperature measurements can be seen in Figure A.4 including the chosen bearing housing temperature $T_{bh}$.

As a brief introduction, heat transfer between two objects $a$ and $b$ can appear in three different forms; convection, conduction and radiation. Convection is heat transfer between a surface and a moving fluid, conduction takes place when a temperature gradient appears in a solid and radiation is electromagnetic waves emitted by a body. The different heat transfers are expressed in the following equations

$$\dot{Q}_{cv,a-b} = hA(T_a - T_b) \tag{3.49}$$

$$\dot{Q}_{cd,a-b} = \frac{\lambda A}{d}(T_a - T_b) \tag{3.50}$$

$$\dot{Q}_{rd,a-b} = \epsilon\sigma(T_a^4 - T_b^4) \tag{3.51}$$

where $h$ is the heat transfer coefficient, $A$ is the area, $\lambda$ is the thermal conductivity, $d$ is the thickness, $\epsilon$ is the emissivity and $\sigma$ is the Stefan–Boltzmann constant.

### 3.9.1 Convection between gas and turbine

To start the determination of occurring heat transfers, the focus is first put on the component exposed to highest temperatures, thus referring to the turbine. Hot exhaust gases from the burner enter through the turbine inlet, hurls around in the turbine volute with a temperature of $T_{03}$, expands in the diffuser to a temperature of $T_{04}$ and then continues out through the outlet. During the described process, it is assumed that most of the heat transfer takes place in the volute with the motivation that it has the largest contact surface area towards the gas and the gas temperature is the highest there.

The heat transferred from the gas to the turbine housing through convection, $\dot{Q}_{cv,g-t}$, is determined by an energy balance with a control volume around the turbine. Using maps with varying turbine inlet temperatures, the convective heat transfer can be calculated as

$$\dot{Q}_{cv,g-t} = \dot{m}_t c_{p,t}(T_{03} - T_{04}) - \dot{W}_{c,adi} - \dot{W}_f \tag{3.52}$$

where $\dot{W}_{c,adi}$ is the adiabatic compressor power, determined by Eq. (3.67)-(3.68). In order to minimize temperature measurement uncertainties described more closely by Franzke et al. [2014], operating points with higher mass flows ($\dot{m}_t > 0.04\,\frac{kg}{s}$) are used in the calculations. With the heat transfer quantified, the convective heat transfer is expressed as

$$\dot{Q}_{cv,g-t} = hA_{g-t}(T_{03} - T_t) \tag{3.53}$$

where $A_{g-t}$ is the internal turbine area exposed to the gas. The heat transfer coefficient $h$ for forced convection is defined as

$$h = \frac{Nu\lambda}{D_{g-t}} \tag{3.54}$$

$$Nu = c_0 Re^{c_1} Pr^{c_2} \tag{3.55}$$

$$Re = \frac{U_\infty D_{g-t}}{\nu} \tag{3.56}$$

$$U_\infty = \frac{\dot{V}_t}{A'_{g-t}}, \qquad \dot{V}_t = \frac{\dot{m}_t R T_{03}}{p_{03}} \tag{3.57}$$

where $Nu$ is the Nusselt number, $\lambda$ is the thermal conductivity, $D_{g-t}$ is the internal diameter, $Re$ is the Reynolds number, $Pr$ is the Prandtl number, $\nu$ is the kinematic viscosity, $U_\infty$ is the free flow velocity, $\dot{V}_t$ is the turbine volume flow and $A'_{g-t}$ is the internal cross-sectional area. Combining Eq. (3.53)-(3.57) and merging all constant values into one constant $c$ yields

$$\dot{Q}_{cv,g-t} = c \cdot (\dot{V}_t/\nu)^{c_1} \lambda Pr^{c_2} (T_{03} - T_t) \tag{3.58}$$

where Prandtl's number, thermal conductivity and kinematic viscosity for air are found in Figure A.5, showing their relationship to temperature. By approximating the volute as a circular tube and using exponential constants proposed by the Sieder-Tate correlation ($c_1 = \frac{4}{5}$, $c_2 = \frac{1}{3}$), the constant $c$ can be estimated using least squares. The resulting model fit can be seen in Figure 3.11 which shows an approximate linear relationship and validates that the model represent the measurements roughly.

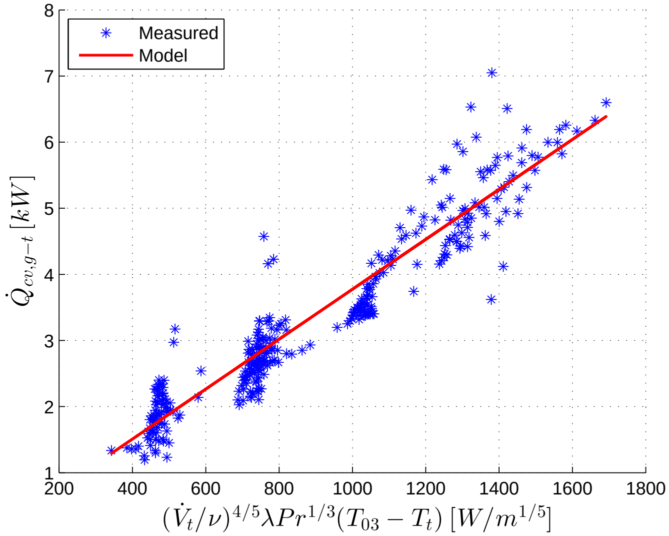

***Figure 3.11:*** *Model versus measurements for the convective heat transfer from the gas to the turbine housing. The figure shows an approximate linear dependency for the measurements with a model that follows roughly.*

### 3.9.2 Conduction between turbine and bearing housing

At steady state operating points, the heat transferred from the gas to the turbine $\dot{Q}_{cv,g-t}$ equals the internal conductive heat transfer $\dot{Q}_{cd,t-bh}$ and the external heat transfer $\dot{Q}_{t-ext}$ as

$$\dot{Q}_{cv,g-t} = \dot{Q}_{cd,t-bh} + \dot{Q}_{t-ext} \tag{3.59}$$

To quantify the conductive heat transfer occurring between the turbine and bearing housing $\dot{Q}_{cd,t-bh}$, measurements where the compressor housing temperature and bearing housing temperature approximately equals ambient temperature ($T_c \approx T_{bh} \approx T_{amb}$) are used. This allows for the conclusion that no heat transfer occurs between the compressor and bearing housing, i.e. all energy transferred to the oil and water, except for the friction heat, is transferred through conduction from the turbine to the bearing housing, hence

$$\dot{Q}_{cd,t-bh} = \dot{Q}_{oil} + \dot{Q}_{wat} - \dot{Q}_f, \qquad \dot{Q}_f = \dot{W}_f \tag{3.60}$$

With calculated heat transfer rate $\dot{Q}_{cd,t-bh}$, the equation for conductive heat transfer yields

$$\dot{Q}_{cd,t-bh} = \frac{\lambda A_{t-bh}}{d_{t-bh}}(T_t - T_{bh}) = c \cdot (T_t - T_{bh}) \tag{3.61}$$

where the constant $c$ is estimated using least squares. The resulting model fit can be seen in Figure 3.12 which shows that the model indicates the quantity roughly. The approximate result is most probably caused by an inaccurate estimation of the bearing housing temperature $T_{bh}$ for some operating points.

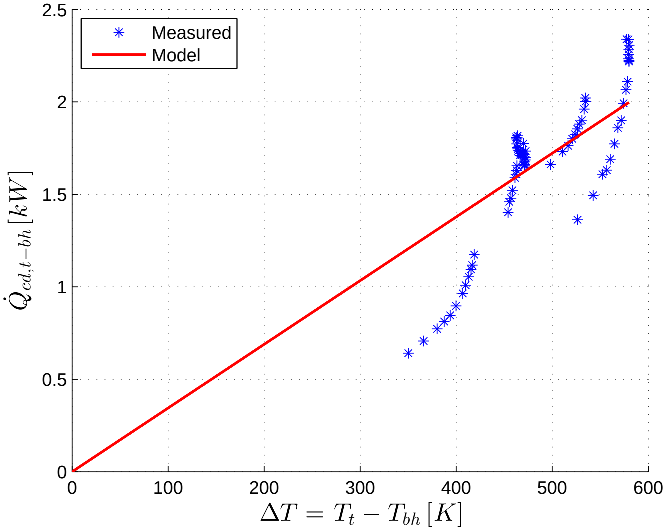

***Figure 3.12:*** *Heat flow through conduction between turbine and bearing housing, model versus measurements. The model gives an approximate estimation of the measurements.*

### 3.9.3 External heat loss of turbine

With a developed model for the conduction between the turbine and bearing housing, the external heat losses $\dot{Q}_{t-ext}$ can be calculated by an energy balance around the turbine, expressed in Eq. (3.62). Steady state measurements with varying turbine inlet temperatures are used in the calculations and the convective heat transfer $\dot{Q}_{cv,g-t}$ is determined by Eq. (3.52).

$$\dot{Q}_{t-ext} = \dot{Q}_{cv,g-t} - \dot{Q}_{cd,t-bh} \tag{3.62}$$

With the assumption that the external heat loss mainly consists of convective heat transfer, the external heat loss $\dot{Q}_{t-ext}$ can be defined as

$$\dot{Q}_{t-ext} = \dot{Q}_{cd,t-ext} + \dot{Q}_{cv,t-ext} + \dot{Q}_{rd,t-ext} = c \cdot (T_t - T_{amb}) \tag{3.63}$$

where the constant $c$ is estimated using least squares. The resulting model fit can be seen in Figure 3.13.

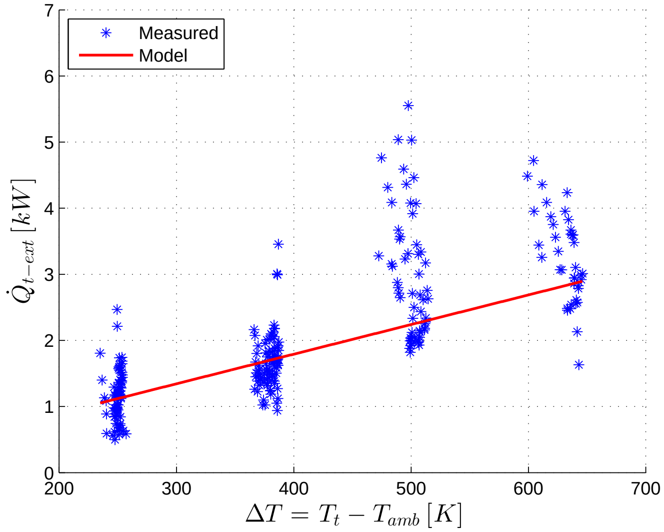

***Figure 3.13:*** *Model versus measurements for the external heat loss of the turbine housing. The poor fit for higher temperature differences is probably the result of an improper estimation of the conduction between the turbine and bearing housing.*

An approximate linear relationship is found in Figure 3.13 resulting in a decent model fit. Some of the measurements exceeding $\Delta T > 450\,K$ does not appear to be linearly dependent. An explanation to this could be that the assumed bearing housing temperature $T_{bh}$ is faulty for some operating points, thus leading to an improperly estimated conduction between the turbine and bearing housing.

### 3.9.4 Conduction between bearing housing and compressor

With a given model for the conductive heat transfer between the turbine and bearing housing, a given friction model and measurements of the heat transferred to the fluids, the conduction between the bearing housing and compressor can be determined by following energy balance with a control volume around the bearing housing

$$\dot{Q}_{cd,bh-c} = \dot{Q}_{cd,t-bh} + \dot{Q}_f - \dot{Q}_{oil} - \dot{Q}_{wat} \tag{3.64}$$

The equation for conduction yields

$$\dot{Q}_{cd,bh-c} = \frac{\lambda A_{bh-c}}{d_{bh-c}}(T_{bh} - T_c) = c \cdot (T_{bh} - T_c) \tag{3.65}$$

where the lumped constant $c$ is estimated using least squares with the resulting model fit presented in Figure 3.14.

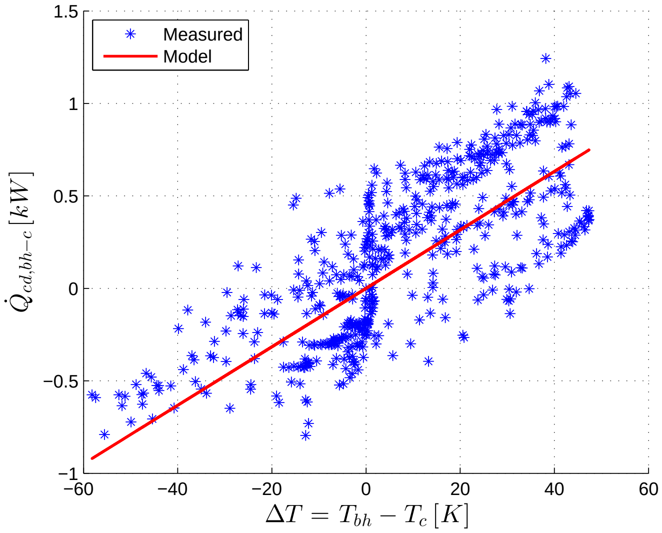

***Figure 3.14:*** *Heat flow through conduction between bearing housing and compressor. The model represent the measurements roughly.*

The model fit is not perfect, but it catches the approximate magnitude which is considered sufficient. As discussed, a better estimation of the bearing housing temperature would most probably lead to a better result.

### 3.9.5 Convection between gas and compressor

Compression of a gas increases its temperature, naturally leading to convective heat transfer between the gas and compressor housing. In the turbocharger, the compressed and heated air is led through the diffuser where most of the convective heat transfer is assumed to take place.

To quantify the heat transfer, the adiabatic efficiency model becomes useful. Since the adiabatic compressor efficiency allows for calculation of the energy supplied to the gas without any heat transfer involved, the difference between the estimated adiabatic power and the actual power utilized defines the convective heat transfer from the gas to the compressor housing as

$$\dot{Q}_{cv,g-c} = \dot{W}_{c,adi} - \dot{m}_c c_{p,c}(T_{02} - T_{01}) \tag{3.66}$$

where the adiabatic power is calculated by the following equations

$$T'_{02} = T_{01} + \frac{T_{01}}{\eta_{c,adi}}\left(\frac{p_{02}}{p_{01}}^{\frac{\gamma_c-1}{\gamma_c}} - 1\right) \tag{3.67}$$

$$\dot{W}_{c,adi} = \dot{m}_c c_{p,c}(T'_{02} - T_{01}) \tag{3.68}$$

In contrast to the convective heat transfer occurring in the turbine, it is here assumed that the kinematic viscosity and thermal conductivity holds a constant value. This is done since the temperature of the compressed air on the compressor side varies within a smaller interval compared to the turbine inlet temperature. Using Eq. (3.54)-(3.57) combined with the mentioned assumptions, an expression for the convective heat transfer $\dot{Q}_{cv,g-c}$ can be derived as

$$\dot{Q}_{cv,g-c} = hA(T'_{02} - T_c) = [\nu, \lambda \; constant] = c \cdot \dot{V}_c^{c_1} Pr^{c_2}(T'_{02} - T_c) \tag{3.69}$$

Since there only is a slight temperature difference $\Delta T = T'_{02} - T_c$ in the steady state measurements, the choice of using time-resolved step response measurement data is done. The constants $c_1$ and $c_2$ are set similarly as for the turbine ($c_1 = \frac{4}{5}, c_2 = \frac{1}{3}$) and the constant $c$ is estimated using least squares. The obtained model fit is presented in Figure 3.15 with satisfying result, showing a clear linear relationship.

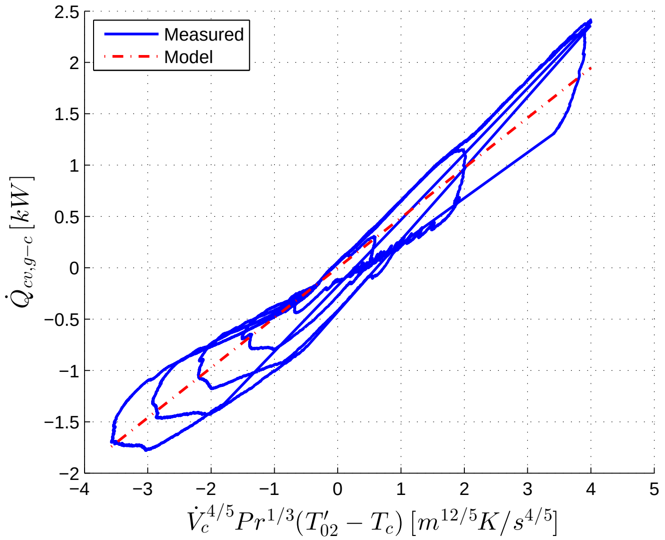

***Figure 3.15:*** *Heat flow through convection between gas and compressor for time-resolved measurements. The model used shows a satisfying fit when comparing with the measurement data.*

For a better understanding the model is displayed against steady state measurement data in Figure 3.16, where it is easy to conclude that the measurements does not show the same clear relationship as in Figure 3.15.

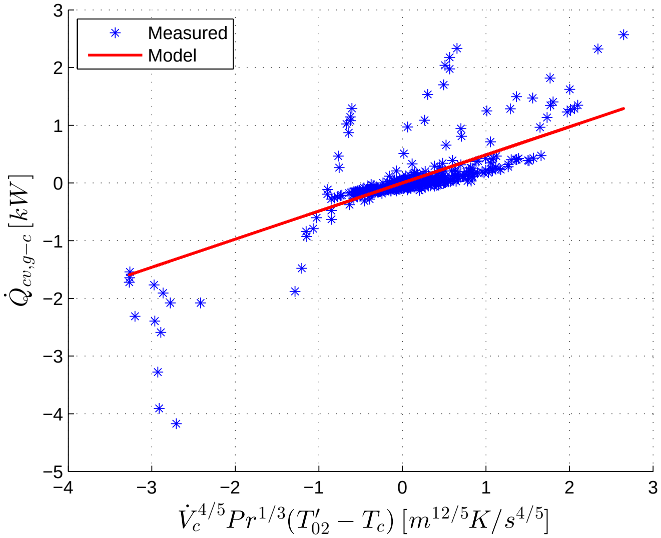

***Figure 3.16:*** *Heat flow through convection between gas and compressor housing, the model developed using time-resolved measurement data displayed against steady state measurements.*

### 3.9.6 External heat loss of compressor

Using steady state measurements and a control volume around the compressor housing, the rate of external compressor heat transfer $\dot{Q}_{c-ext}$ can be determined by an energy balance expressed as

$$\dot{Q}_{c-ext} = \dot{Q}_{cv,g-c} + \dot{Q}_{cd,bh-c} \tag{3.70}$$

Since the compressor temperature reaches a maximum temperature of $180°C$ during all measurements, radiative heat transfer is assumed to be negligible. By assuming that the external heat loss is linearly dependent of the temperature difference $\Delta T = T_c - T_{amb}$, following model is proposed

$$\dot{Q}_{c-ext} = c \cdot (T_c - T_{amb}) \tag{3.71}$$

The constant $c$ is adjusted in order to match the simulated compressor housing temperature to the measured. This is done since it is impossible to interpret a linear relationship of the measured data seen in Figure 3.17. When comparing with the measurements, the adjusted model seems reasonable since it represent the measurements in an approximate way. The measurements for higher turbocharger speeds ($N_{tc} > 96\,000\,rpm$) appears to be odd. An explanation for the discrepancy is that the adiabatic compressor efficiency model fit is insufficient for higher turbocharger speeds as discussed, resulting in a faulty estimation of the convective heat transfer $\dot{Q}_{cv,g-c}$.

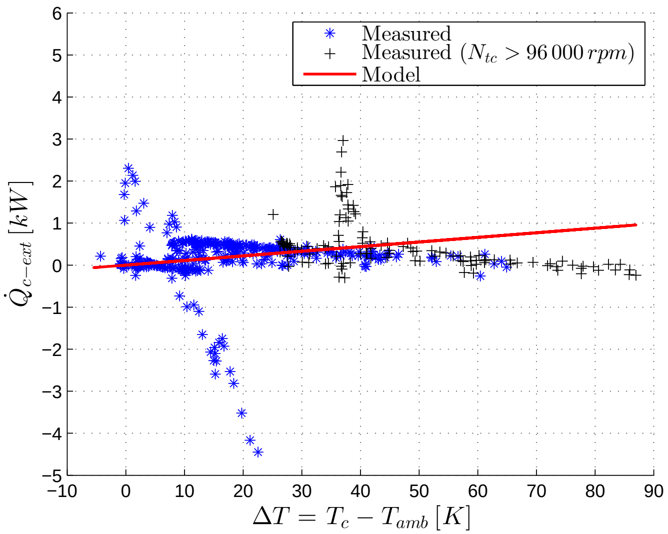

***Figure 3.17:*** *Model versus measurements for the external heat loss of the compressor. The outliers for higher speeds is the result of a poor model fit regarding the adiabatic compressor efficiency model.*

### 3.9.7 Convection between bearing housing and oil

The main purpose of the oil circuit is to lubricate the turbocharger bearing, but since the fluid is flowing through the bearing housing, heat transfer between the housing and oil is made possible. With available measurements of oil temperature before and after passing through the turbocharger and measurements of mass flow rate, the energy transferred to the oil can be calculated as

$$\dot{Q}_{oil} = \dot{m}_{oil} c_{p,oil} (T_{oil,out} - T_{oil,in}) \tag{3.72}$$

The equation for convection yields

$$\dot{Q}_{oil} = hA(T_{bh} - T_{oil}) = [\lambda, Pr, \nu\ constant] = c_1 \dot{V}^{c_2} (T_{bh} - T_{oil}) \tag{3.73}$$

where Prandtl's number $Pr$, thermal conductivity $\lambda$ and kinematic viscosity $\nu$ for the oil is assumed to be constant since the temperature is fairly constant. The constant $c_2$ is manually adjusted to achieve a linear relationship and the lumped constant $c_1$ is then estimated using least squares. The model fit can be seen in Figure 3.18 which shows that the model follows the measurements roughly. The result is considered sufficient since the objective is to develop models that captures the general characteristic of each heat transfer.

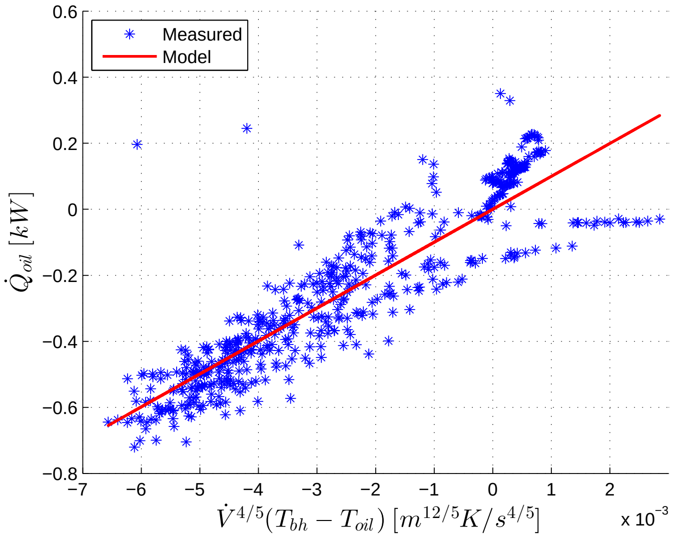

***Figure 3.18:*** *Model versus measurements for the convective heat transfer between bearing housing and compressor shows that the model approximately represent the measurements.*

### 3.9.8 Convection between bearing housing and water

The water circuit has the purpose of cooling the turbocharger, thus leading to a longer life time for the component. Same modeling approach as used for the convection between bearing housing and oil is applied here, expressed in Eq. (3.74)-(3.75) below

$$\dot{Q}_{wat} = \dot{m}_{wat} c_{p,wat} (T_{wat,out} - T_{wat,in}) \tag{3.74}$$

$$\dot{Q}_{wat} = hA(T_{bh} - T_{wat}) = [\lambda, Pr, \nu \ constant] = c_1 \dot{V}^{c_2} (T_{bh} - T_{wat}) \tag{3.75}$$

where $c_2 = \frac{4}{5}$ and $c_1$ is estimated using least squares with the model fit shown in Figure 3.19. The result indicates that something is wrong because it is impossible to identify a linear relationship.

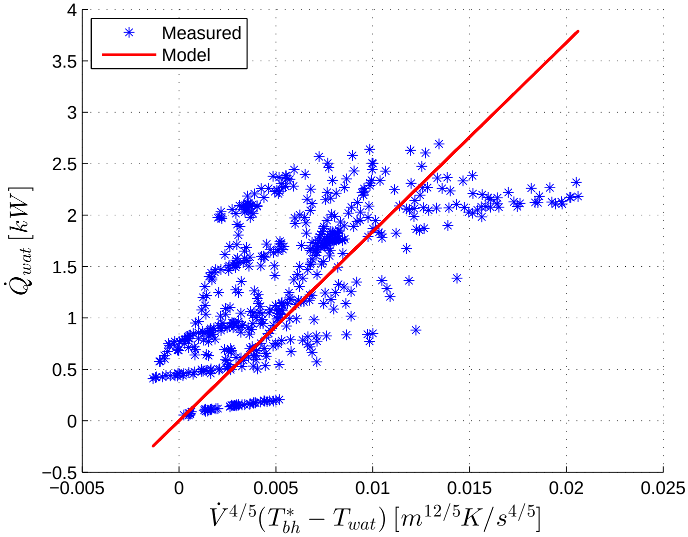

***Figure 3.19:*** *Heat flow through conduction between bearing housing and compressor, model versus measurements. The poor result indicates that another method is required.*

As mentioned earlier, no measurements were conducted on the actual bearing housing. Since the model is not depending on a lot of variables, the first guess would be that it is the represented bearing housing temperature $T_{bh}$ that is causing the poor model fit. By assuming that the actual bearing housing temperature is dependent on the turbine housing temperature $T_t$ as well, a new representation of the bearing housing temperature is defined as

$$T^*_{bh} = \frac{T_{bh} + T_t}{2} \tag{3.76}$$

The constant $c_1$ in Eq. (3.75) is once again estimated using least squares and the resulting model fit can be seen in Figure 3.20.

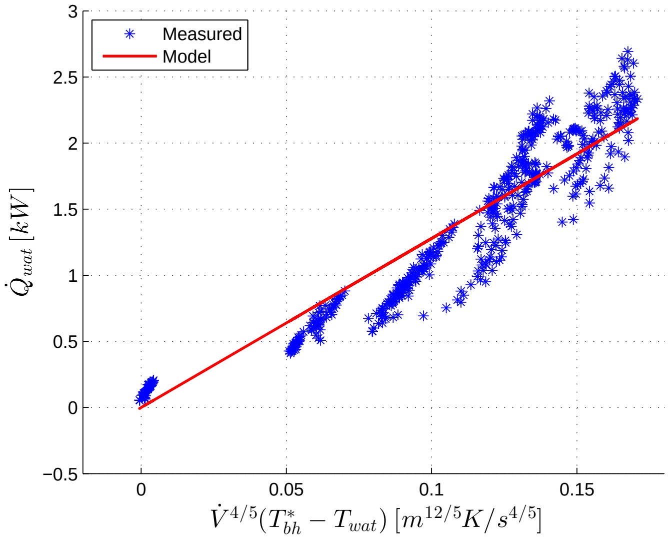

***Figure 3.20:*** *The new model versus measurements for the conductive heat transfer between bearing housing and compressor. The figure shows an improved model fit.*

When comparing the result in Figure 3.20 with the model fit presented in Figure 3.19, one can easily see that the new model is an improvement. It is possible that an even better result can be obtained by including temperature-dependent oil properties. However, the developed model is considered to give a good enough estimation.

### 3.9.9 Thermal mass

Mass acts like an inertia against temperature variations, which is expressed in the equation below

$$\frac{dT}{dt} = \frac{1}{mc_p}\sum \dot{Q} \tag{3.77}$$

where $m$ is the mass and $c_p$ is the heat capacity at constant pressure. Used material parameters in Simulink are $c_{p,alu} = 0.91\,\frac{kJ}{kgK}$ for the compressor and $c_{p,ci} = 0.46\,\frac{kJ}{kgK}$ for both the turbine and bearing housing. The masses are adjusted in order to match simulated and measured data, with the following results

$$m_c = 4\,kg, \quad m_{bh} = 4\,kg, \quad m_t = 9\,kg$$

which seems reasonable when comparing them to each other.

## 3.10 Complete Model Validation

With mathematical models describing each component respectively, they are all implemented and connected in Simulink for a complete model validation. An overview of the final Simulink model can be seen in Figure 3.21.

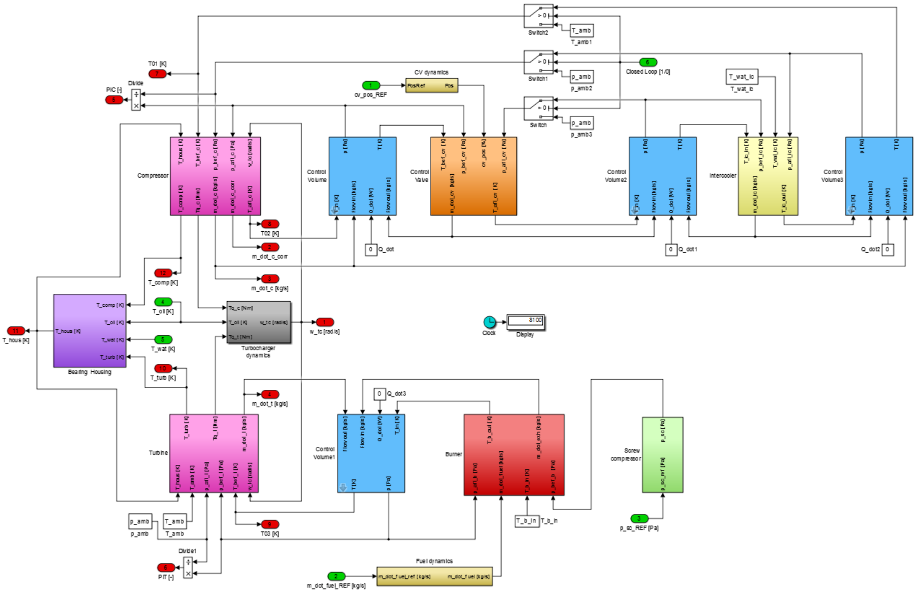
T01 [K]
PIC [-]
Divide
CV dynamics
PosRef
Pos
cv_pos_REF
Switch2
T_amb
T_amb1
Switch1
p_amb
p_amb2
Switch
p_amb
p_amb3
Closed Loop [1/0]
T_wat_ic
T_wat_ic
Compressor
T_hous [K]
T_bef_c [K]
p_bef_c [Pa]
p_aft_c [Pa]
w_tc [rad/s]
T_comp [K]
Tq_c [Nm]
m_dot_c [kg/s]
m_dot_c_corr
T_aft_c [K]
Control Volume
p [Pa]
T [K]
T_in [K]
Flow in [kg/s]
Q_dot [W]
Flow out [kg/s]
Control Valve
T_bef_cv [K]
p_bef_cv [Pa]
cv_pos [%]
p_aft_cv [Pa]
m_dot_cv [kg/s]
T_aft_cv [K]
Control Volume2
Intercooler
T_ic_in [K]
p_bef_ic [Pa]
T_wat_ic [K]
p_aft_ic [Pa]
m_dot_ic [kg/s]
T_ic_out [K]
Control Volume3
T02 [K]
m_dot_c_corr
Q_dot
Q_dot1
Q_dot2
T_comp [K]
m_dot_c [kg/s]
T_oil [K]
w_tc [rad/s]
Tq_t [Nm]
Turbocharger dynamics
T_hous [K]
T_wat [K]
T_turb [K]
Bearing Housing
Clock
8100
Display
m_dot_t [kg/s]
Q_dot3
Turbine
T_turb [K]
Tq_t [Nm]
m_dot_t [kg/s]
T_amb [K]
p_aft_t [Pa]
p_bef_t [Pa]
T_bef_t [K]
Control Volume1
Burner
T_b_out [K]
m_dot_exh [kg/s]
p_aft_b [Pa]
m_dot_fuel [kg/s]
T_b_in [K]
p_bef_b [Pa]
Screw compressor
p_sc [Pa]
p_sc_ref [Pa]
p_amb
T_amb
T03 [K]
T_b_in
p_sc_REF [Pa]
Divide1
PIT [-]
Fuel dynamics
m_dot_fuel_ref [kg/s]
m_dot_fuel [kg/s]
m_dot_fuel_REF [kg/s]

***Figure 3.21:*** *An overview of the gas stand Simulink model. Block colours together with descriptions: Pink - Compressor & turbine, Grey - Turbocharger dynamics, Purple - Bearing housing, Orange - Butterfly valve, Red - Burner, Green - Screw compressor, Yellow - Intercooler, Blue - Control volume.*

The model is controlled by two PI controllers, one controlling the turbocharger speed by adjusting the screw compressor pressure and one controlling the turbine inlet temperature by adjusting the fuel supplied to the burner. The regulator parameters are reversed engineered in order to maintain the same conditions in the simulation environment as during the measurements, thus allowing for a better validation.

Used reference signals for the PI controllers during the simulation are the predefined steps in turbocharger speed together with a constant turbine inlet temperature of 600°$C$. The control valve is set to a fixed position, manually adjusted to match the simulated compressor pressure ratio to the measured. This is done since the control valve position is not available in the time-resolved measurement data. The same applies for the oil and water volume flows which are thus adjusted in order to match the simulated bearing housing temperature to the measured. When comparing the adjusted values with the steady state measurement data, they seems to be reasonable. Oil and water temperatures are available in the time-resolved data and are thus defined similarly in Simulink. The result of the simulation is presented against measured data in Figure 3.22 and Figure 3.23.

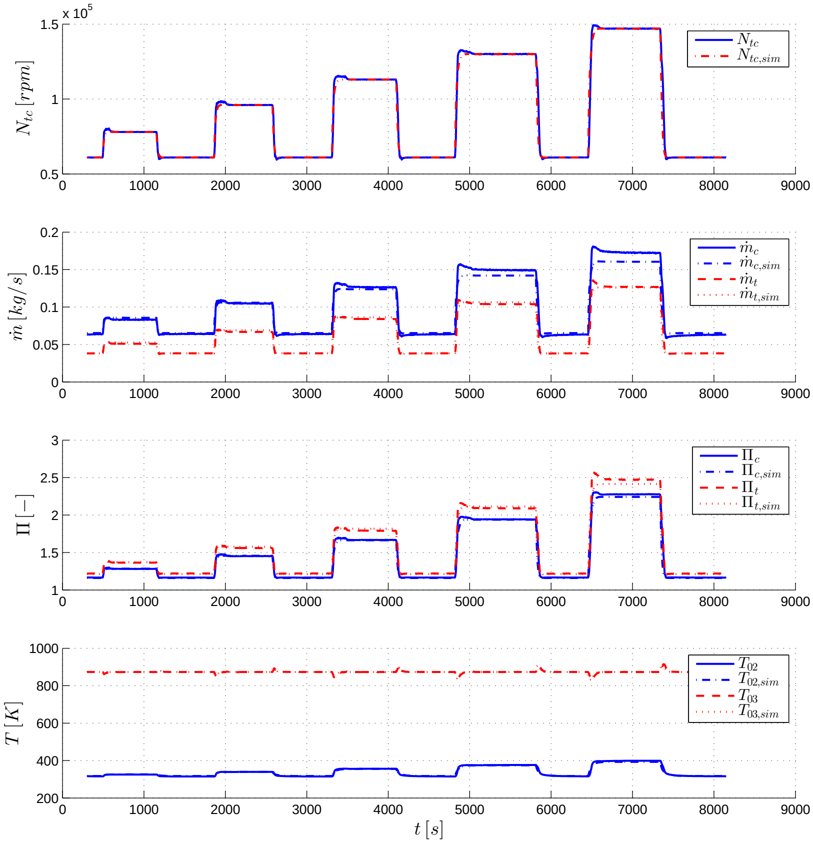

***Figure 3.22:*** *Measured and simulated data for the speed, mass flow rates, pressure ratios and temperatures over time. The figure shows that all the simulated data follows the measurements within a reasonable distance.*

Since the objective when developing all models has been to reach a good enough model fit and not necessarily a perfect one, the result seen in Figure 3.22 is considered satisfying. Most of the simulated values follow the corresponding measurements closely. The only misfit seen in the figure is the simulated compressor flow for higher turbocharger speeds, which is reasonable since the compressor flow model is inaccurate for higher speeds.

Figure 3.23 shows that the simulated values for the turbine temperature is close to a perfect fit against measurements. The same behaviour applies for the compressor temperature $T_c$ with the exception for the highest speed, which is the result of a faulty estimated compressor efficiency and compressor flow. Concerning the simulated bearing housing temperature, it is not really a validation against measurements. Although, it validates that it is possible to obtain similar behaviour as the measured temperature with reasonable volumes flows used in the simulation environment.

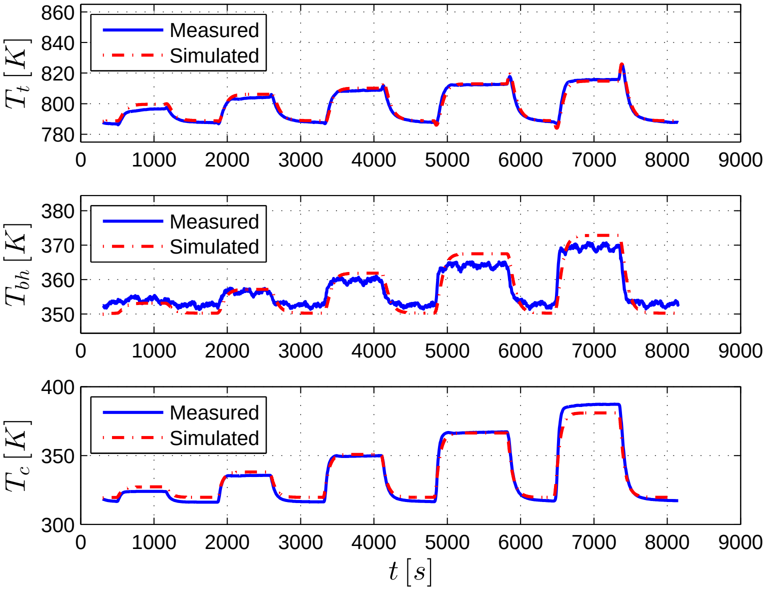

***Figure 3.23:*** *Measured and simulated turbocharger temperatures for the turbine, bearing housing and compressor over time. The figure validates that the heat transfer models are decent since the simulated values follow the measurements within reasonable distance.*

# 4

# Control

To speed up the otherwise time consuming and costly process of turbo mapping, this chapter investigates if an added component to the gas stand can contribute in terms of making the mapping procedure more time efficient. Instead of testing possible solutions on the physical gas stand, the validated gas stand model in Simulink allows for an investigation in the simulation environment.

When measuring a steady state map point, it is required that the parameters of interest are stabilized before a measurement is conducted, thus referring to turbocharger speed, pressure ratio, mass flow and efficiency. Since temperatures of the turbocharger components affect the measured quantities, the component needs to reach a thermal equilibrium before a measurement can be conducted.

In this study, the focus is put on speeding up the compressor mapping procedure, and more specifically the determination of efficiency. The question to answer is if it is possible to decrease the time of reaching a thermal equilibrium with the help of an external heat source, e.g. an infrared heater.

Compressor efficiency is defined by Eq. (3.2) and includes the compressor pressure ratio $\Pi_c$, inlet temperature $T_{01}$ and outlet temperature $T_{02}$. Since it is assumed that the inlet temperature is constant in the Simulink model and the pressures are controllable in a faster way compared to the temperatures, the parameter of interest here is the outlet temperature $T_{02}$. The target is to stabilize it as fast as possible using an added idealized heat source in the Simulink model with the possibility to heat up the compressor housing. The heat source is controlled by a PI controller with feedback of $T_{02}$, using predefined values as reference.

Figure 4.1 compares the results of two different step responses with steps made in reference turbocharger speed, one with an added controlled heat source and one without. The result shows that with the help of an added heat source with a power capacity of 1 $kW$, the compressor efficiency reaches an equilibrium roughly 200 seconds faster in comparison to the original case.

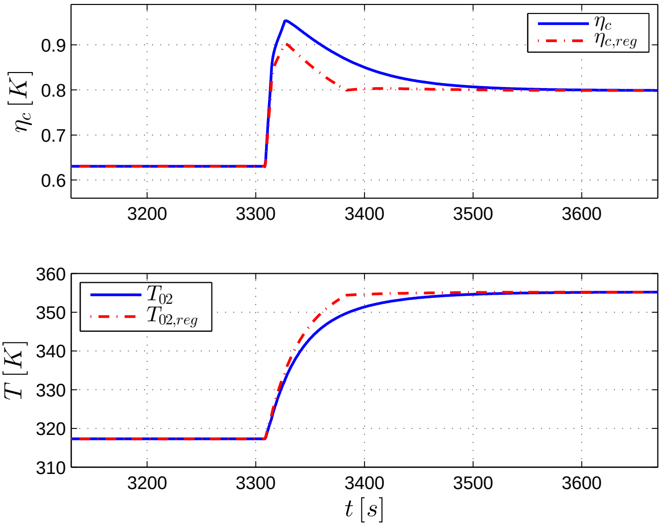

***Figure 4.1:*** *Compressor efficiency $\eta_c$ and compressor outlet temperature $T_{02}$ over time. The abbreviation reg means that the compressor housing has been heated with an external heat source in Simulink with a power capacity of 1 $kW$. The figure shows that when a heat source is added, the settling time for the efficiency measurement is reduced.*

Heat sources of varying power capacities are tested and the relation between power capacity and possible time to save when switching between two steady state points is presented in Table 4.1. The results show that there is a lot of potential time to save only by using a control strategy with focus on the thermal aspects.

| Power [$kW$] | Time saved [$s$] |
|---:|:---:|
| 0.2 | 140 |
| 0.5 | 180 |
| 1 | 200 |
| 2 | 230 |
| 4 | 240 |

***Table 4.1:*** *The relation between power capacity of an extra heat source and possible time to save when changing between two steady state measurements.*

# 5

# Conclusions and Future Work

A 0D model of a gas stand has been developed and implemented in Simulink in order to allow for development of an enhanced control strategy used when mapping turbochargers. Each gas stand component is modeled and validated against available measurement data, all showing a reasonable result. Turbocharger heat transfers have been studied and modeled with varying validation result. The imprecise results is most probably the cause of unavailable measurements of the bearing housing temperature, leading to a vague estimation of the actual temperature. Since some of the heat transfer models are determined by energy balances, a slight error in one heat transfer model will influence others.

After connecting all gas stand sub models including turbocharger heat transfers, a complete model validation shows that the model works properly. With a working simulation model, an improvement of the test procedure is examined by means of adding an extra heat source with the possibility to heat the compressor housing. The study shows that a lot of time can be saved when changing between two operating points during steady state measurements, since it is possible to reach a thermal equilibrium faster.

Suggestions of model improvements and other possible future work topics are found in the following list

- Improve the adiabatic compressor efficiency model.
- Investigate the turbocharger heat transfers further.
- Include heat transfers associated with the control volumes and burner.
- Develop an enhanced control strategy using the original gas stand configuration only.

# Appendix

# A

# Appendix

# Measurement Data

Steady state measurement data is shown in Figure A.1 and time-resolved data from step responses carried out is shown in Figure A.2.

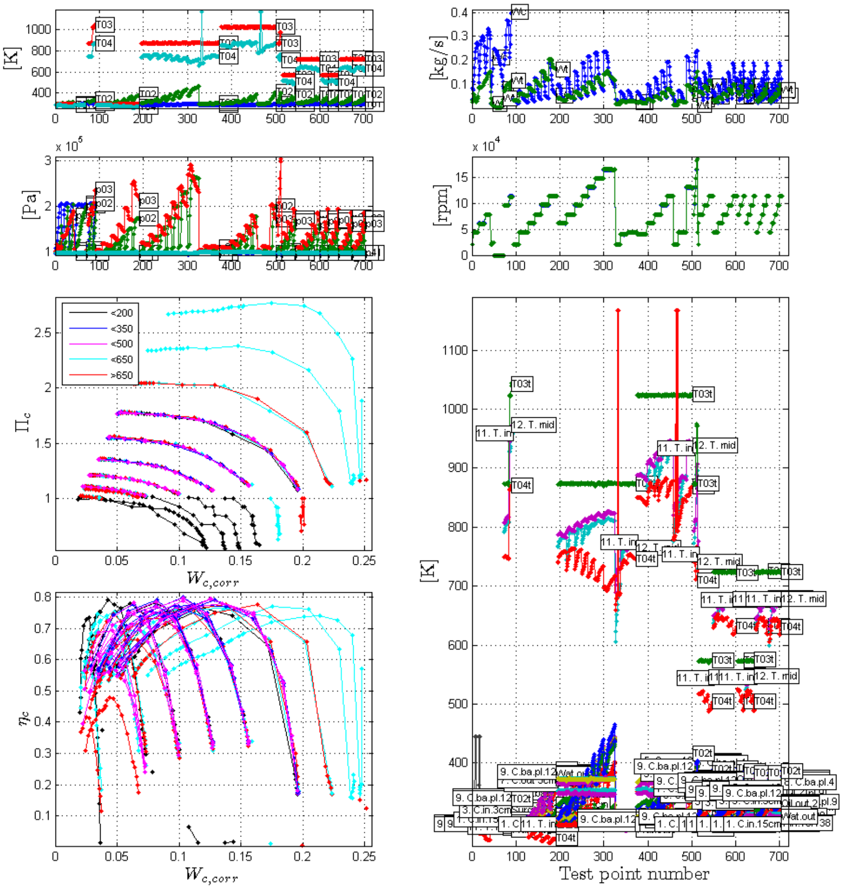

*Figure A.1: Steady state measurement data from all conducted measurements.*

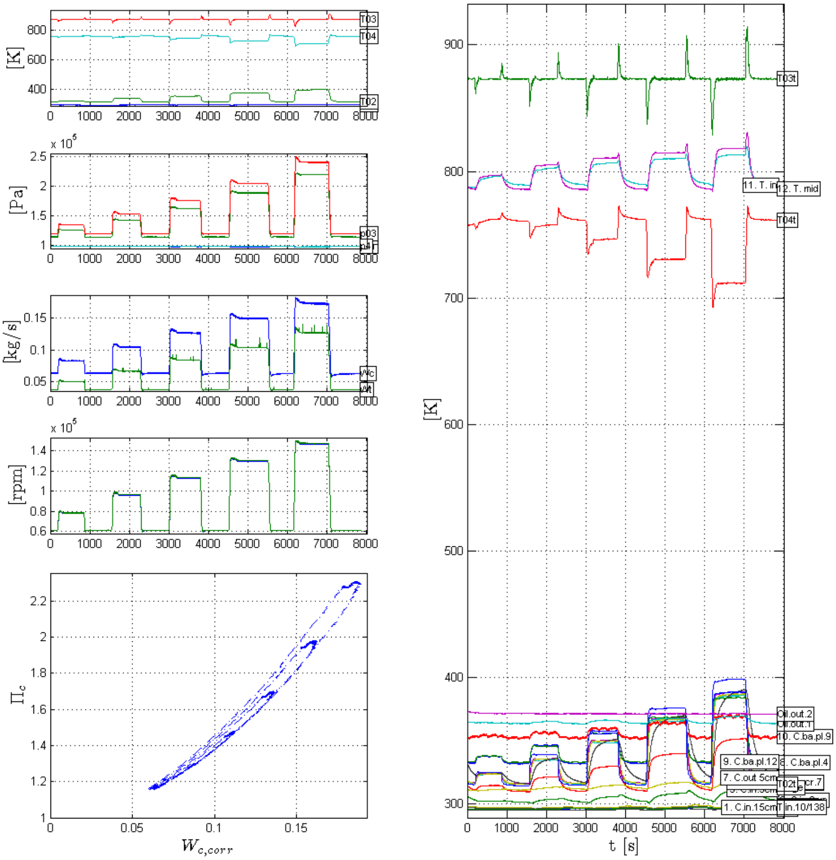

***Figure A.2:*** *Data from step responses carried out with steps made in turbocharger reference speed.*

# Oil Properties

Oil properties used in the turbocharger friction model are shown in Figure A.3.

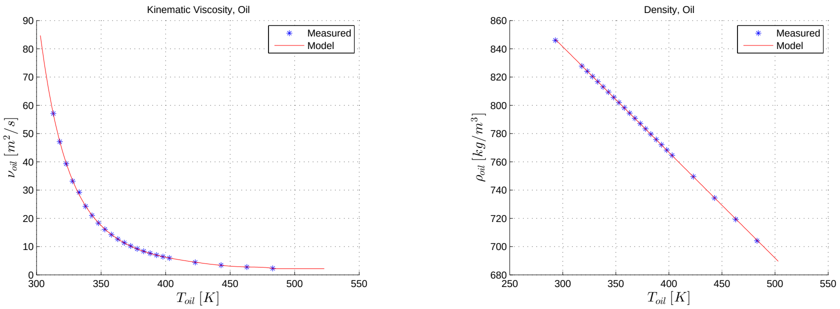

***(a)** Kinematic viscosity of oil.*

***(b)** Oil density.*

***Figure A.3:** Oil properties as functions of temperature.*

## Turbocharger Temperatures

Steady state measurements from the thermocouples placed on the turbocharger surface is shown i Figure A.4.

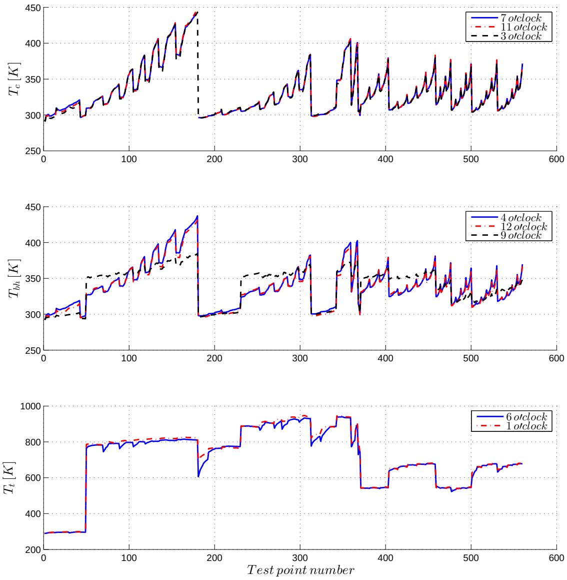

***Figure A.4:** Turbocharger housing temperatures from the conducted steady-state measurements. It is decided that the bearing housing temperature $T_{bh}$ is represented by the thermocouple placed 9 o'clock on the compressor back plate.*

# Air Properties

Figure A.5 shows how the air properties used in the convection calculations vary with temperature.

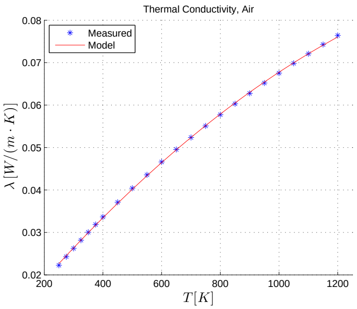

***(a)*** *Thermal conductivity of air.*

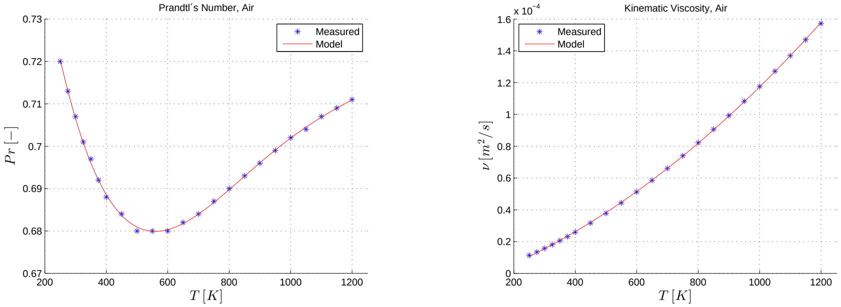

***(b)*** *Prantdl's number of air.*

***(c)*** *Kinematic viscosity of air.*

***Figure A.5:*** *Air properties as functions of temperature.*

# Notation

## NOMENCLATURE

| Symbol | Meaning |
|---|---|
| $A$ | Area $[m^2]$ |
| $c_d$ | Drag coefficient $[-]$ |
| $c_p$ | Heat capacity at constant pressure $[J/(kg \cdot K)]$ |
| $c_v$ | Heat capacity at constant volume $[J/(kg \cdot K)]$ |
| $d$ | Diameter $[m]$ |
| $h$ | Heat transfer coefficient $[W/(m^2 \cdot K)]$ |
| $J$ | Moment of inertia $[kg \cdot m^2]$ |
| $\dot{m}$ | Mass flow $[kg/s]$ |
| $N$ | Rotational speed $[rpm]$ |
| $Nu$ | Nusselt number $[-]$ |
| $p$ | Pressure $[Pa]$ |
| $Pr$ | Prandtl's number $[-]$ |
| $q$ | Heating value $[J/kg]$ |
| $Q$ | Heat $[J]$ |
| $\dot{Q}$ | Heat transfer rate $[W]$ |
| $r$ | Radius $[m]$ |
| $R$ | Ideal gas constant $[J/(kg \cdot K)]$ |
| $Re$ | Reynolds number $[-]$ |
| $T$ | Temperature $[K]$ |
| $Tq$ | Torque $[Nm]$ |
| $U$ | Velocity $[m/s]$ |
| $V$ | Volume $[m^3]$ |
| $\dot{W}$ | Power $[W]$ |
| $\Pi$ | Pressure ratio $[-]$ |
| $\gamma$ | Heat capacity ratio $[-]$ |
| $\epsilon$ | Emissitivity $[-]$ |
| $\eta$ | Efficiency $[-]$ |
| $\lambda$ | Thermal conductivity $[W/(m \cdot K)]$ |
| $\mu$ | Dynamic viscosity $[kg/(m \cdot s)]$ |
| $\nu$ | Kinematic viscosity $[m^2/s]$ |
| $\xi$ | Effectiveness $[-]$ |
| $\rho$ | Density $[kg/m^3]$ |
| $\sigma$ | Stefan–Boltzmann constant $[J/(m^2 \cdot s \cdot K^4)]$ |
| $\omega$ | Angular speed $[rad/s]$ |

## ABBREVATIONS

| Abbrevation | Meaning |
|---|---|
| adi | adiabatic |
| aft | after |
| alu | aluminium |
| amb | ambient |
| bef | before |
| BSR | Blade Speed Ratio |
| b | bearing |
| bh | bearing housing |
| bv | butterfly valve |
| bu | burner |
| c | compressor |
| cd | conduction |
| ci | cast iron |
| cv | convection |
| co | corrected |
| exh | exhaust |
| ext | external |
| f | friction |
| fu | fuel |
| g | gas |
| ic | intercooler |
| LHV | Lower Heating Value |
| rd | radiation |
| ref | reference |
| t | turbine |
| tc | turbocharger |
| TFP | Turbine Flow Parameter |
| wat | water |
| $\infty$ | free flow |

# Bibliography

SAE J1826 Mar. 1995. Turbocharger gas stand test code. URL `http://www-cs-faculty.stanford.edu/~{}uno/abcde.html`. Cited on page 2.

Per Andersson. *Air Charge Estimation in Turbocharged Spark Ignition Engines*. PhD thesis, Linköpings Universitet, December 2005. Cited on page 23.

Massimo Capobianco and Silvia Marelli. Transient performance of automotive turbochargers: Test facility and preliminary experimental analysis. In *SAE Technical Paper*. Consiglio Nazionale delle Ricerche, 09 2005. doi: 10.4271/2005-24-066. URL `http://dx.doi.org/10.4271/2005-24-066`. Cited on page 3.

L. Eriksson and L. Nielsen. *Modeling and Control of Engines and Drivelines*. Automotive Series. Wiley, 2014. ISBN 9781118536209. URL `https://books.google.se/books?id=jS34AgAAQBAJ`. Cited on pages 12, 16, 18, and 23.

Fernando Antonio Rodrigues Filho, Ramón Molina Valle, José Eduardo Mautone Barros, and Sérgio de Morais Hanriot. Automotive turbocharger maps building using a flux test stand. In *SAE Technical Paper*. SAE International, 11 2002. doi: 10.4271/2002-01-3542. URL `http://dx.doi.org/10.4271/2002-01-3542`. Cited on page 3.

B. Franzke, B. Höpke, D. Lückmann, R. Aymanns, and T. Uhlmann. Impact of temperature measurement and turbine heat loss on turbocharger performance characteristics. *Aufladetechnischen Konferenz*, 19(23), 2014. Cited on page 25.

Oskar Leufven. *Modeling for control of centrifugal compressors*. PhD thesis, Linköping University, 2013. Cited on page 6.

Oskar Leufven and Lars Eriksson. Engine test bench turbo mapping. In *SAE Technical Paper*. SAE International, 04 2010. doi: 10.4271/2010-01-1232. URL `http://dx.doi.org/10.4271/2010-01-1232`. Cited on page 3.

J. M. Luján, V. Bermúdez, J. R. Serrano, and C. Cervelló. Test bench for turbocharger groups characterization. In *SAE Technical Paper*. SAE International, 03 2002. doi: 10.4271/2002-01-0163. URL `http://dx.doi.org/10.4271/2002-01-0163`. Cited on page 2.

Detlef Naundorf, Holger Bolz, and Michael Mandel. Design and implementation of a new generation of turbo charger test benches using hot gas technology. In *SAE Technical Paper*. SAE International, 03 2001. doi: 10.4271/2001-01-0279. URL `http://dx.doi.org/10.4271/2001-01-0279`. Cited on page 2.

P. Olmeda, V. Dolz, F.J. Arnau, and M.A. Reyes-Belmonte. Determination of heat flows inside turbochargers by means of a one dimensional lumped model. *Mathematical and Computer Modelling*, 57(7–8):1847 – 1852, 2013. ISSN 0895-7177. doi: http://dx.doi.org/10.1016/j.mcm.2011.11.078. URL `http://www.sciencedirect.com/science/article/pii/S0895717711007631`. Cited on page 3.

Alessandro Romagnoli and Ricardo Martinez-Botas. Heat transfer analysis in a turbocharger turbine: An experimental and computational evaluation. *Applied Thermal Engineering*, 38(0):58 – 77, 2012. ISSN 1359-4311. doi: http://dx.doi.org/10.1016/j.applthermaleng.2011.12.022. URL `http://www.sciencedirect.com/science/article/pii/S1359431111007198`. Cited on page 3.

Jose Serrano, Pablo Olmeda, Francisco Arnau, and Artem Dombrovsky. General procedure for the determination of heat transfer properties in small automotive turbochargers. *SAE Int. J. Engines*, 8:30–41, 10 2014. doi: 10.4271/2014-01-2857. URL `http://dx.doi.org/10.4271/2014-01-2857`. Cited on page 3.

Eric Stemler and Patrick Lawless. The design and operation of a turbocharger test facility designed for transient simulation. In *SAE Technical Paper*. SAE International, 02 1997. doi: 10.4271/970344. URL `http://dx.doi.org/10.4271/970344`. Cited on page 2.

H. Tu and H. Chen. Modeling of a compressor's performance map by fitting function methodology. *Advanced Materials Research*, 779-780:1194 – 1198, 2013. ISSN 0895-7177. doi: http://10.4028/www.scientific.net/AMR.779-780.1194. Cited on page 10.

Greg Uhlenhake, Ahmet Selamet, Kevin Fogarty, Kevin Tallio, and Philip Keller. Development of an experimental facility to characterize performance, surge, and acoustics in turbochargers. In *SAE Technical Paper*. SAE International, 05 2011. doi: 10.4271/2011-01-1644. URL `http://dx.doi.org/10.4271/2011-01-1644`. Cited on page 3.

Giuliano Gardolinski Venson, Jose Eduardo Mautone Barros, and Josemar Figueiredo Pereira. Development of an automotive turbocharger test stand using hot gas. In *SAE Technical Paper*. SAE International, 11 2006. doi: 10.4271/2006-01-2680. URL `http://dx.doi.org/10.4271/2006-01-2680`. Cited on page 2.

N. Watson and S. Janota. *Turbocharging the Internal Combustion Engine*. Macmillan, 1982. ISBN 9780333242902. URL `https://books.google.se/books?id=JsugQgAACAAJ`. Cited on page 17.

F. Westin. *Accuracy of Turbocharged SI-engine Simulations*. TRITA-MMK. KTH, 2002. Cited on page 18.

Michael Y. Young and David A. Penz. The design of a new turbocharger test facility. In *SAE Technical Paper*. SAE International, 02 1990. doi: 10.4271/900176. URL `http://dx.doi.org/10.4271/900176`. Cited on page 2.

Linköpings universitet

## Upphovsrätt

Detta dokument hålls tillgängligt på Internet — eller dess framtida ersättare — under 25 år från publiceringsdatum under förutsättning att inga extraordinära omständigheter uppstår.

Tillgång till dokumentet innebär tillstånd för var och en att läsa, ladda ner, skriva ut enstaka kopior för enskilt bruk och att använda det oförändrat för ickekommersiell forskning och för undervisning. Överföring av upphovsrätten vid en senare tidpunkt kan inte upphäva detta tillstånd. All annan användning av dokumentet kräver upphovsmannens medgivande. För att garantera äktheten, säkerheten och tillgängligheten finns det lösningar av teknisk och administrativ art.

Upphovsmannens ideella rätt innefattar rätt att bli nämnd som upphovsman i den omfattning som god sed kräver vid användning av dokumentet på ovan beskrivna sätt samt skydd mot att dokumentet ändras eller presenteras i sådan form eller i sådant sammanhang som är kränkande för upphovsmannens litterära eller konstnärliga anseende eller egenart.

För ytterligare information om Linköping University Electronic Press se förlagets hemsida `http://www.ep.liu.se/`

## Copyright

The publishers will keep this document online on the Internet — or its possible replacement — for a period of 25 years from the date of publication barring exceptional circumstances.

The online availability of the document implies a permanent permission for anyone to read, to download, to print out single copies for his/her own use and to use it unchanged for any non-commercial research and educational purpose. Subsequent transfers of copyright cannot revoke this permission. All other uses of the document are conditional on the consent of the copyright owner. The publisher has taken technical and administrative measures to assure authenticity, security and accessibility.

According to intellectual property law the author has the right to be mentioned when his/her work is accessed as described above and to be protected against infringement.

For additional information about the Linköping University Electronic Press and its procedures for publication and for assurance of document integrity, please refer to its www home page: `http://www.ep.liu.se/`

© Mikael Bengtsson